Lamellar Bodies of Human Epidermis : Proteomics Characterization by High Throughput Mass Spectrometry and Possible Involvement of CLIP-170 in their Trafficking/Secretion

Anne-Aurélie Raymond, Anne Gonzalez de Peredo, Alexandre Stella, Akemi Ishida-Yamamoto, David Bouyssié, Guy Serre, Bernard Monsarrat, Michel Simon

Lamellar Bodies of Human Epidermis

PROTEOMICS CHARACTERIZATION BY HIGH THROUGHPUT MASS SPECTROMETRY AND POSSIBLE INVOLVEMENT OF CLIP-170 IN THEIR TRAFFICKING/SECRETION*[S]

Anne-Aurélie Raymond‡§, Anne Gonzalez de Peredo¶, Alexandre Stella¶, Akemi Ishida-Yamamoto‖, David Bouyssie¶, Guy Serre‡, Bernard Monsarrat¶, and Michel Simon‡**

Lamellar bodies (LBs) are tubulovesicular secretory organelles of epithelial cells related to lysosomes. In the epidermis, they play a crucial role in permeability barrier homeostasis, secreting their contents, lipids, a variety of hydrolases, protease inhibitors, and antimicrobial peptides, in the upper keratinocyte layers. The identification of proteins transported in epidermal LBs is still far from complete, and the way their secretion is controlled unknown. In this study, we describe the first proteomics characterization by nano-LC-MS/MS of a fraction enriched in epidermal LBs. We identified 984 proteins, including proteins known or thought to be secreted by LBs. Moreover 31 proteins corresponded to lysosomal components further suggesting that LBs are a new class of secretory lysosomes. Many of the newly found proteins could play a role in the epidermal barrier and desquamation (one acid ceramidase-like protein, apolipoproteins, glycosidases, protease inhibitors, and peptidases) and in LB trafficking (*e.g.* Rab, Arf, and motor complex proteins). We focus here on CLIP-170/restin, a protein that mediates interactions between organelles and microtubules. Western blotting confirmed the presence of CLIP-170 and its known effectors IQGAP1 and Cdc42 in the LB-enriched fraction. We showed, by confocal microscopy analysis of skin cryosections, that CLIP-170 was expressed in differentiated keratinocytes, first at the periphery of the nucleus then with a granular cytoplasmic labeling evocative of LBs. It was preferentially co-localized with Cdc42 and with the known LB protein cathepsin D. CLIP-170 was also largely co-localized with Rab7. This study strongly suggests a new function for CLIP-170, its involvement together with Cdc42 and/or Rab7 in the intracellular trafficking of LBs, and provides evidence that nano-LC-MS/MS combined with monodimensional electrophoresis separation constitutes a powerful method for identifying proteins in a complex mixture such as subcellular structures. ***Molecular & Cellular Proteomics 7: 2151–2175, 2008.***

Terminal differentiation of keratinocytes is a program of gene expression oriented from the basal layer to the surface of the epidermis. Keratinocytes express specific proteins in a sequential manner and undergo a series of structural and metabolic modifications resulting in the formation of corneocytes. The accumulation of these cells forms the stratum corneum and establishes a protective permeability barrier (1). Secretory structures called lamellar bodies (LBs)[1] or keratinosomes are crucial to stratum corneum homeostasis and barrier function. As observed by classical electron microscopy, LBs are round or oblong membrane-delimited and lamellate organelles measuring 0.1–0.5 μm in diameter. Recent cryotransmission electron microscopy studies have revealed that LBs are rather branched tubulovesicular structures derived from the trans-Golgi network (2). Moreover Norlen (2) has proposed that membranes of the trans-Golgi network and of LBs and the keratinocyte plasma membrane may well be part of one and the same continuous membrane structure. The observations that LBs contain lysosomal enzymes like cathepsin D (3, 4) and vacuolar H^+-ATPase and have acidic contents (5) have led them to be considered as lysosome-related organelles. They are produced in the keratinocytes of the upper stratum spinosum and are more abundant in the cytoplasm of the granular keratinocytes (6, 7). They secrete their contents, lipids (glucosylceramides, sphingomyelin, phospholipids, and cholesterol) and lipid-processing enzymes (*e.g.* β-glucocerebrosidase also known as glucosylceramidase, acid sphingomyelinase, and secretory phospho-

From the ‡UMR5165 CNRS-University of Toulouse III, Institut Fédératif de Recherche Claude de Préval (INSERM-CNRS-Université Paul Sabatier-Centre Hospitalier Universitaire de Toulouse) 31059 Toulouse, France, ¶UMR5089 CNRS-University of Toulouse III, Institute of Pharmacology and Structural Biology, 31077 Toulouse, France, and ‖Department of Dermatology, Asahikawa Medical College, Asahikawa 078-8510, Japan

Received, July 23, 2007, and in revised form, June 12, 2008

Published, MCP Papers in Press, July 12, 2008, DOI 10.1074/mcp.M700334-MCP200

[1] The abbreviations used are: LB, lamellar body; ABCA, ATP-binding cassette transporter; IIF, indirect immunofluorescence; IP, immunoprecipitation; OMIM, Online Mendelian Inheritance in Man; H + L, heavy plus light; 1D, one-dimensional; cps, counts/s; MFPaQ, Mascot File Parsing and Quantification; LAMP, lysosome-associated membrane protein; Arf, ADP-ribosylation factor; SNARE, soluble *N*-ethylmaleimide-sensitive factor attachment protein receptor; t-SNARE, target SNARE; v-SNARE, vesicle SNARE; VAMP, vesicle-associated membrane protein; NSF, *N*-ethylmaleimide-sensitive factor; SNAP, soluble NSF attachment protein; Vps, vacuolar protein sorting; CLIP, cytoplasmic linker protein; IQGAP1, IQ motif-containing GTPase-activating protein 1.

lipase A_2) that make the upper layers waterproof (8, 9), structural proteins like corneodesmosin that optimizes corneocyte cohesion (10), proteases (kallikreins and cathepsins), glycosidases and protease inhibitors (*e.g.* elafin, secretory leucocyte protease inhibitor, lympho-epithelial kazal-type-related inhibitor, and α_2-macroglobulin-like) involved in the control of desquamation (11, 12), and antimicrobial peptides (defensins and cathelicidin) (13, 14), at the stratum granulosum/stratum corneum interface. The secreted proteins seem to be delivered by independent trafficking of various cargoes (4). Recently Sando *et al.* (15) have shown an enrichment of caveolin-1 in an isolated LB fraction and have confirmed the location of caveolin-1 in LBs by immunoelectron microscopy, suggesting that caveolins may play a role in LB assembly, trafficking, and/or function.

LB secretion is often increased to correct an impaired epidermal barrier function, including recovery from adhesive stripping, repair of experimental wounds (16), and psoriasis (17). Defective delivery of LB content has been noted in atopic dermatitis, leading to a significant increase of their volume in the transition zone between the stratum granulosum and the stratum corneum (18). The LB lipid transporter ABCA12 is underexpressed in harlequin ichthyosis (OMIM 242500), resulting not only in reduced transfer of lipids to LBs but also in abnormal delivery of enzymes to the stratum corneum extracellular spaces. This induces profound abnormalities in the stratum corneum and epidermal barrier and a delay in desquamation (19, 20).

Organelles morphologically similar to LBs have been observed in other tissues implicated in the establishment of a barrier between the organism and the environment: mucosa of the gastrointestinal tract, the vermilion border of the lip, tongue papillae, and occasionally in the epithelium of the cervix (21, 22). LBs of pneumocytes are the organelles for surfactant secretion into the alveolar lumen of the lung, reducing surface tension at the air-liquid interface and preventing collapse of the organ during expiration (23). Interestingly mutations of *ABCA3* are associated with respiratory distress syndrome (OMIM 267450) (24), suggesting common or similar pathways between epidermal and lung epithelium LBs.

The identification of proteins transported by epidermal LBs and of their constitutive components is still far from complete, and little is known about the molecular mechanisms involved in their trafficking. Rab11, a small GTPase involved in recycling endosomes, has been co-localized with known LB molecules, including glucosylceramides, corneodesmosin, and cathepsin D, suggesting that it could play a role in the intracellular trafficking of various types of LBs to the cell surface (25).

In this study, we analyzed a fraction enriched in epidermal LBs by LC-MS/MS, and then we focused on CLIP-170/restin, a protein described previously as mediating interactions between organelles and microtubules and being involved in vesicular trafficking (26). By confocal microscopy analysis, we showed that CLIP-170, together with one of its effectors, was localized on a subpopulation of LBs in normal human epidermis.

EXPERIMENTAL PROCEDURES

Human Tissues—All the studies described concerning human tissues were conducted in accordance with the Declaration of Helsinki and with the ethical guidelines of both the University of Toulouse III and the French Ministry of Research and Technology. Normal human breast skin fragments were obtained from patients without any history of skin diseases undergoing plastic surgery and after informed consent. They were provided by Prof. J.-P. Chavoin (Plastic Surgery Department, Rangueil Teaching Hospital, Toulouse, France).

Subcellular Fractionation—The method we used to prepare a fraction enriched in LBs (supplemental Fig. 1) closely followed that described previously (15). Dermoepidermal cleavage was performed by heat treatment. The subsequent steps were performed at 4 °C. Epidermis from 100 cm^2 of skin was minced with scissors and disrupted by a loose fitting Teflon-glass Potter-Elvehjem homogenizer in 40 ml of homogenization buffer (20 mM sodium phosphate, pH 6.5, 0.15 M NaCl, 10 mM EDTA, 1 mM phenylmethylsulfonyl fluoride, 2 μg/ml pepstatin, 2 μg/ml aprotinin, 2 μg/ml leupeptin, and 10 mM 2-mercaptoethanol). The homogenate was centrifuged for 15 min at 800 $\times$ *g* to remove cell debris, and the supernatant obtained (S1) was centrifuged for 30 min at 20,000 $\times$ *g*. The 20,000 $\times$ *g* supernatant was centrifuged again for 30 min at 100,000 $\times$ *g* to obtain the S100 cytosolic fraction. The 20,000 $\times$ *g* pellet was washed in 40 ml of homogenization buffer, centrifuged again for 30 min at 20,000 $\times$ *g*, reconstituted in 1 ml of homogenization buffer, and layered onto a preformed linear density gradient of 20–50% Optiprep (Sigma). After centrifugation for 2 h at 26,000 $\times$ *g*, we observed three opaque bands at the top, middle, and bottom of the gradient. The upper band was collected and filtered through a 0.8-μm-pore size polyethersulfone membrane filter (Millipore Corp.) to get the LB-enriched fraction.

Proteins of the LB-enriched fraction were diluted into 10 ml of homogenization buffer and either centrifuged for 15 min at 15,000 $\times$ *g* for electron microscopy analysis or precipitated with 10% trichloroacetic acid for separation by SDS-PAGE. To obtain the Tris-EDTA-Nonidet P-40 epidermis extract, after dermoepidermal cleavage had been performed by heat treatment, the epidermis was extracted in a Tris-EDTA buffer containing 0.5% Nonidet P-40 as reported previously (27). Protein concentrations were measured using the Bio-Rad protein assay.

Antibodies—The characteristics of the antibodies used in the study are summarized in Table I.

Protein Electrophoresis and Immunoblotting—Proteins were separated by SDS-PAGE on 7.5 or 12.5% acrylamide gels (7 or 12 cm long) and electrotransferred to nitrocellulose membranes. The membranes were stained with Ponceau Red, then incubated for 30 min in blocking buffer (TBS (40 mM Tris-HCl, pH 8, and NaCl 0.9%) supplemented with 0.5% low fat dried milk and 0.05% Tween 20), and probed with antibodies as described previously (27). Immunoreactivities were revealed with an ECL™ Western blotting kit as recommended by the manufacturer (GE Healthcare).

Electron Microscopy—For ultrastructural studies by standard electron microscopy, whole skin or the pelleted LB-enriched fraction was fixed in 0.1 M cacodylate-buffered 3% formaldehyde, 3% glutaraldehyde overnight at 4 °C and postfixed in 1% osmium tetroxide with 1.5% potassium ferrocyanate in 0.2 M cacodylate buffer at pH 6.8. After rinsing and dehydration through an ascending acetone series, the tissues were embedded in LR White resin (SPI Supplies, West Chester, PA). Thin sections were stained with uranyl acetate and examined in a Hitachi HU12A electron microscope.

Immunoelectron microscopy using Lowicryl HM20 resin (Chemische Werke Lowi, Waldkraiburg, Germany) and ultrathin cryosections was performed as described previously with a rabbit anti-KLK7 antibody (4). Negative controls included incubations with unrelated

TABLE I
Source and properties of polyclonal and monoclonal antibodies used in this study

Antigen	Supplier[a]	Catalog number	Antibody type,[b] clone	Dilution for WB[c]	Dilution for IIF
Caspase-14	SC	sc-5628	R	1:5,000	NR[d]
Cathepsin D	O	IM16	R	NR	1:20
Caveolin-1	TL	610059	R	1:30,000	NR
Cdc42	CS	2462	R	1:1,000	1:40
Corneodesmosin	Homemade (31)	NR	R, $B_{102-115}$	NR	1:10
Corneodesmosin	Homemade (10)	NR	M, G36-19	NR	1:250
Corneodesmosin	Homemade (10)	NR	M, F28-27	1:2,500	NR
CLIP-170	SC	sc-28325	M, F3	1:500	1:300
IQGAP1	SC	sc-10792	R	1:5,000	1:80
Kallikrein-7	Homemade (31)	NR	R, SCCE-B	1:500	NR
Kallikrein-8	RD	MAB1719	M, 189004	1:250	NR
Rab7	SC	sc-10767	R	1:500	1:40
CLIP-170	SC	sc-12799	G, N18	NR	1:40
α-Tubulin	Abcam	15-246	R	NR	1:1,000

[a] CS, Cell Signaling Technology; O, Oncogen; SC, Santa Cruz Biotechnology; RD, R&D Systems; TL, BD Transduction Laboratories.
[b] R, rabbit polyclonal antibody; M, mouse monoclonal antibody; G, goat polyclonal antibody.
[c] Western blot.
[d] NR, not relevant.

primary antibodies. Secondary antibodies were 5-nm gold-conjugated goat anti-rabbit IgG (GE Healthcare).

Indirect Immunofluorescence—Indirect immunofluorescence (IIF) was performed on unfixed 4-μm-thick cryosections of breast skin samples blocked with PBS containing 4% goat serum and 0.05% Tween 20 and then incubated with primary antibodies diluted in PBS containing 2% goat serum and 0.05% Tween 20 for 1 h at 37 °C or overnight at 4 °C. The sections were washed twice in PBS containing 0.05% Tween 20 and twice in PBS and then incubated for 1 h at room temperature with the secondary antibody (Alexa Fluor 488 goat anti-mouse IgG (H + L), Alexa Fluor 555 goat anti-rabbit IgG (H + L), or Alexa Fluor 488 donkey anti-goat IgG (H + L), Molecular Probes, Eugene, OR) diluted to 1: 400 in PBS containing 2% goat serum and 0.05% Tween 20. After two washes in PBS containing 0.05% Tween 20 and two washes in PBS, nuclei were stained with Toto-3 iodide (1:1000; Molecular Probes) for 30 min at room temperature. The sections were washed in distilled water and eventually mounted in an antifading solution (Mowiol, Calbiochem) before observation under a confocal laser microscope (LSM 510, Carl Zeiss, Oberkochen, Germany). For negative controls, sections were incubated without primary antibodies. Results were analyzed using the NIS-Element AR 2.30 software (Nikon, Tokyo, Japan). In particular, co-localization was evaluated by a comparison of the emission spectra of the fluorochromes along a line crossing several stained structures. This was performed to analyze all, at least 100 (the exact number is indicated by "*n*"), of the stained structures on one focal plan.

Analysis by 1D Gel/Nano-LC-MS/MS—One hundred micrograms of proteins of the LB-enriched fraction were resuspended in 40 mM Tris-HCl, pH 7.5, and 6 M urea and incubated for 30 min at room temperature after addition of Laemmli buffer. Proteins of the S100 fraction were directly incubated after addition of Laemmli buffer. Proteins of both fractions were alkylated in 90 mM iodoacetamide for 30 min at room temperature, separated by SDS-PAGE on 12.5% acrylamide short gels (7 cm long), and detected by Coomassie Blue staining. The entire gels were cut into 16 homogeneous slices. Alternatively 200 μg of proteins prepared in the same conditions were separated on 12-cm-long gels that were cut into 55 slices.

Gel slices were separately washed and then digested with modified sequencing grade trypsin (Promega, Madison, WI), and the resulting peptides were extracted following established protocols (28). The resulting peptides were analyzed by nano-LC-MS/MS using an LC Packings system (Dionex, Amsterdam, Netherlands) coupled to a QSTAR XL mass spectrometer (Applied Biosystems). Dried peptides were reconstituted in 12 μl of solvent A′ (5% acetonitrile and 0.05% trifluoroacetic acid in HPLC grade water), and 6 μl were loaded onto a precolumn (300-μm inner diameter × 5 mm) using the Switchos unit of the LC Packings system, delivering a flow rate of 20 μl/min of solvent A′. After desalting for 7 min, the precolumn was switched on line with the analytical column (75-μm inner diameter × 15 cm, PepMap C_{18}) equilibrated in 95% solvent A (5% acetonitrile and 0.1% formic acid in HPLC grade water) and 5% solvent B (95% acetonitrile and 0.1% formic acid in HPLC grade water). Peptides were eluted from the precolumn to the analytical column and then to the mass spectrometer with a gradient from 5 to 50% solvent B for 80 min at a flow rate of 200 nl/min delivered by the Ultimate pump. The QSTAR XL was operated in information-dependent acquisition mode with the Analyst QS 1.1 software. MS and MS/MS data were recorded continuously with a 5-s cycle time. Within each cycle, MS data were accumulated for 1 s over the mass range *m/z* 300–2000 followed by two MS/MS acquisitions of 2 s each on the two most abundant ions over the mass range *m/z* 80–2000. Dynamic exclusion was used within 60 s to prevent repetitive selection of the same ions. Collision energies were automatically adjusted according to the charge state and mass value of the precursor ions. The MS to MS/MS switch threshold was set to 10 cps.

Database Searching—The Mascot Daemon software (Mascot Daemon version 2.1.6, Matrix Science, London, UK) was used to automatically extract peak lists from Analyst .wiff files and to perform database searches in batch mode with all the .wiff files acquired on each gel slice. For peak list creation, the default charge state was set to 2+, 3+, and 4+. MS and MS/MS centroid parameters were set to 50% height percentage and a merge distance of 0.1 amu. All peaks in MS/MS spectra were conserved (threshold intensity set to 0% of highest peak). For MS/MS grouping, the following averaging parameters were selected: reject spectra with less than five peaks or precursor ions with less than 5 cps or more than 10,000 cps; the precursor mass tolerance for grouping was set to 0.1 Da, the maximum number of cycles per group was set to 10, and the minimum number of cycles per group was set to 1. MS/MS data were searched against *Homo sapiens* entries in the public database UniProt v7.1, which consists of Swiss-Prot Protein Knowledgebase Release 49.1 and TrEMBL Protein Database Release 32.1 (2,826,393 entries in total, 72,049 human sequences) using the Mascot search engine

(Mascot Daemon version 2.1.6, Matrix Science). Carbamidomethylation of cysteines was set as a fixed modification, and oxidation of methionine and phosphorylation of serine and threonine were set as variable modifications for all Mascot searches. Specificity of trypsin digestion was set for cleavage after lysine or arginine except before proline, and two missed trypsin cleavage sites were allowed. Both the peptide MS and MS/MS tolerances were set to 0.5 Da.

Mascot results were parsed with the in-house developed software Mascot File Parsing and Quantification (MFPaQ) (29), which allows automatic validation of the proteins returned by Mascot according to user-defined criteria and also provides a convenient interface for performing manual validation. All the Mascot result files (.dat files) corresponding to a series of nano-LC-MS/MS analysis (fractions of a 1D gel) were extracted in batch, and protein hits were automatically validated if they satisfied one of the following criteria: identification with at least one top ranking peptide ("red" peptide) with a Mascot score of more than 51 (corresponding to a p value of 0.001, *i.e.* 99.9% identification confidence), or at least two top ranking peptides each with a Mascot score of more than 36 (corresponding to a p value of 0.0316), or at least three top ranking peptides each with a Mascot score of more than 31 (corresponding to a p value of 0.1). These two last validation criteria correspond to a final confidence of $p = 0.001$ if each peptide identification is considered independent. To evaluate the false positive rate in these large scale experiments, we repeated the Mascot searches using identical search parameters against a decoy database and performed MFPaQ parsing on these results using the same criteria. The decoy database was the compilation of UniProt Swiss-Prot and UniProt TrEMBL Databases (same versions as mentioned above) in which the sequences had been reversed. The false positive rate was calculated for each fraction by dividing the number of validated identifications in the reversed database with the number of validated identifications in the forward database. A final percentage of false positives was obtained by averaging the false positive rates obtained for each fraction.

From all the validated result files corresponding to the fractions of a 1D gel lane, MFPaQ was used to generate a unique, non-redundant list of proteins. The software compares proteins or protein groups (composed of all the proteins matching the same set of peptides) and creates clusters from protein groups found in different gel slices if they have one common member. This feature allowed a global list to be edited of unique proteins (or clusters) representing the entire sample analyzed in the experiment.

RESULTS

Preparation of LB-enriched Fraction—An LB-containing fraction was obtained from a human epidermis homogenate with a powerful method using subcellular fractionation and density gradient sedimentation as described previously (15) but with an additional filtration step (supplemental Fig. 1). This step cleared out most of the contamination from large fragments of membranes and melanosomes as observed by electron microscopy (data not shown). The LB-containing fraction obtained was then analyzed by Western blotting, electron microscopy, and immunoelectron microscopy (Fig. 1). Multilamellar vesicles were observed with morphology and size (0.1–0.5 μm in diameter) very similar to those of LBs observed in the entire epidermis (Fig. 1, *a* and *b*). A few vesicles were intact (Fig. 1*b*, *black arrows*), but most of them were damaged and more or less empty (Fig. 1*b*, *open arrows*). To study the efficacy of the enrichment in LBs, equal amounts of proteins of the crude (S1 fraction) and LB-containing fractions were immunodetected using antibodies directed against LB markers caveolin-1, kallikrein-8, and corneodesmosin (Fig. 1*c*). Much higher amounts of caveolin-1 (19- and 22-kDa isoforms) and kallikrein-8 (28 kDa) were detected in the LB-fraction, thus showing the enrichment. Corneodesmosin was also enriched but was largely degraded during the procedure despite the presence of several protease inhibitors. In contrast, high levels of the cytosoluble protein caspase-14 were detected in the S1 fraction at 28 and 17 kDa, the molecular mass of its proform and active form, respectively, but caspase-14 was hardly present in the LB-enriched fraction. In the LB-enriched fraction analyzed by immunoelectron microscopy, we were also able to detect kallikrein-7 (Fig. 1*d*) and dermokine (data

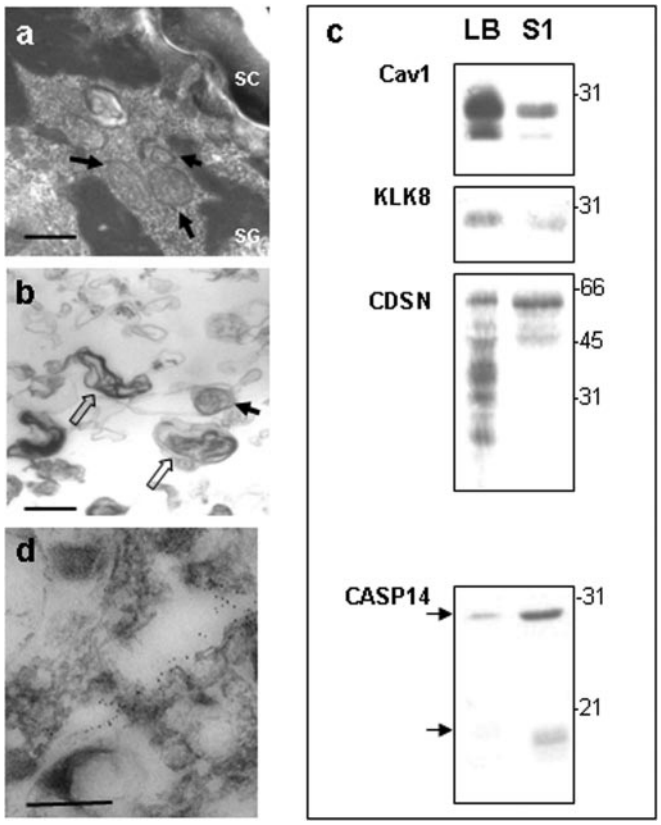

FIG. 1. **Analysis of the LB-containing epidermal fraction.** *a* and *b*, the skin section (*a*) and the LB-containing fraction (*b*) were analyzed by electron microscopy. Note that vesicles in both the intact epidermis and the LB-enriched fraction are in the same size range. Some of them (*black arrows*) have the same lamellar morphology. In the LB-containing fraction, several vesicles are damaged or even empty (*open arrows*). *c*, equal amount of proteins of the S1 and LB-containing fractions were immunodetected with antibodies directed against LB markers caveolin-1 (*Cav1*), kallikrein-8 (*KLK8*), and corneodesmosin (*CDSN*) and against the cytosolic protein caspase-14 (*CASP14*). *Arrows* point to the proform and active form of caspase-14. The position of molecular mass standards (kDa) is indicated on the *left*. *d*, kallikrein-7 was detected in the LB-containing fraction by immunoelectron microscopy (*arrow*). In the presence of irrelevant antibodies, no labeling was observed (not shown). The *bars* correspond to 150 nm in *a* and *b* and 200 nm in *d*.

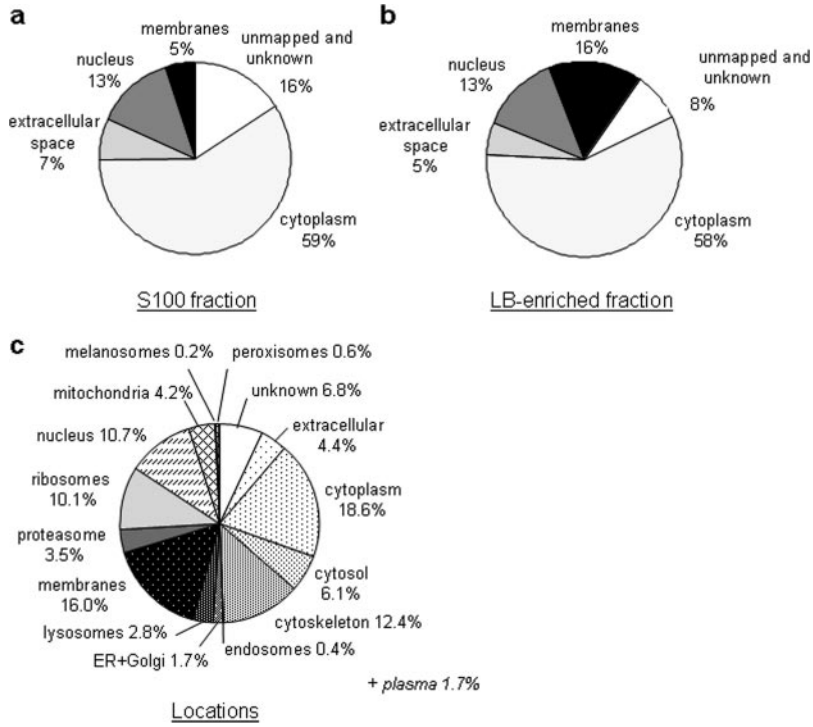

FIG. 2. **Cellular and functional distribution of the proteins identified by the LC-MS/MS analyses.** *a* and *b*, 570 proteins were identified from the S100 fraction, and 467 proteins were identified from the LB-enriched fraction during the first LC-MS/MS analysis (sample fractionated into 16 gel slices). They were sorted automatically with the knowledge-based software developed by Ingenuity Systems Inc. according to their subcellular distribution. *c*, during a second LC-MS/MS identification, 517 additional proteins were identified in the LB-enriched fraction (sample fractionated into 55 gel slices). The 984 non-redundant proteins from the LB-enriched fraction were manually analyzed according to their cellular locations. *ER*, endoplasmic reticulum.

not shown), two other proteins known to be secreted via LB (30, 31). Taken together, these results show that the LB fraction was indeed enriched in LB, allowing further proteomics characterization. Herein it will be referred to as the LB-enriched fraction.

Identification of Proteins by LC-MS/MS Analysis of the LB-enriched Fraction—The LB-enriched fractions prepared from the homogenates obtained from the epidermis of 15 different individuals (~250 cm^2) were pooled. The cytosoluble (S100) fractions were also pooled, and 100 μg of proteins of each pool were separated by monodimensional electrophoresis on two 7-cm-long acrylamide gels. The entire gel lanes were cut into 16 slices, and proteins were digested by trypsin and then identified by nano-LC-MS/MS analysis and Mascot database searches. Mascot result files were parsed automatically, and protein hits were validated using different criteria based on the number, rank, and score of the assigned peptides. Using these criteria, 570 proteins were identified from the S100 fraction, and 467 proteins were identified from the LB-enriched fraction. The lists of proteins corresponding to each sample are provided (supplemental Tables 1 and 2, respectively) together with the lists of peptides identified in each gel slice with their associated MS data (supplemental Tables 4 and 5). Protein identification with a single, top ranking peptide match was validated when the score of this single peptide was higher than 51 ($p < 0.001$), and for these identifications, the corresponding annotated MS/MS spectra are shown in supplemental Fig. 2. With the validation criteria used, the estimated rate of protein false positives from the reversed database search was closed to 0.3%. Among the 467 proteins, 241 were common to both proteomes, whereas 226 were specific to the LB-enriched fraction. A large number of the common proteins corresponded to components of the cytoskeleton and to abundant nuclear, ribosomal, and proteasomal proteins (data not shown). The latter probably correspond to contamination as observed in other high throughput MS proteomics approaches (32). Proteins were sorted according to their subcellular distribution either automatically (Fig. 2, *a* and *b*) with the knowledge-based software developed by Ingenuity Systems Inc. that helps to interpret data sets in the context of biological process and molecular network or manually (data not shown) using several broad (PubMed, ExPASy, Human Protein Reference Database, and EBIMed) and specialized (MEROPS, Secreted Protein Database, and Protein Data Bank of Transmembrane Proteins) databases. Comparable results were obtained with both methods, showing the validity of data obtained with the Ingenuity software. For example, similar percentages of proteins from the LB-enriched fraction were classified as membranous (16 *versus* 17%) and extracellular (5% for both) or were not classified (unmapped and unknown; 8 *versus* 6%). The major discrepancies were noted for cytoplasmic (58 *versus* 62%) and nuclear (13 *versus* 10%) proteins. Confirming the enrichment, 16% of proteins identified in the LB-enriched fraction were automatically sorted as membrane proteins as compared with only 5% of the proteins identified in the S100 fraction.

We noted that two LB markers present in the enriched fraction as shown by Western blotting, corneodesmosin (Fig. 1*c*) and kallikrein-7 (data not shown), were not identified dur-

ing the LC-MS/MS approach. This suggested that other proteins had probably also escaped the MS identification. Complete proteomics analysis of a complex mixture is limited by the sequencing speed of the mass spectrometer as many peptides co-elute from the chromatographic column at any given time and cannot all be selected for MS/MS sequencing. This leads to preferential identification of high abundance components, whereas minor proteins remain undetected. To increase the power of the LC-MS/MS method, we separated twice the amount of proteins (200 μg) of the LB-enriched fraction from another preparation (prepared from 28 different skin samples) on a longer gel and cut the migration lane into 55 slices. Most (89%) of the previously identified proteins were found again, showing the reproducibility of the purification method and of the proteomics analysis. Moreover extensive separation of the proteins of the LB-enriched fraction, resulting in longer analysis time (higher number of nano-LC-MS/MS runs performed on mixtures of lower complexity), allowed the number of MS/MS scans performed by the mass spectrometer and the number of proteins identified to be increased (supplemental Tables 3 and 6). As shown in supplemental Table 3, 517 additional proteins were identified from this experiment. Using the same validation criteria as before, the reversed database search used as a negative control revealed 0.86% false positives. The improvement in the method allowed us to identify more proteins of low abundance, such as enzymes (37% (191 of 517) as compared with 29% (135 of 467)), and of a hydrophobic nature like transmembrane transporters/ion channels (12% (62 of 517) *versus* 8% (37 of 467)). Altogether the two procedures identified 984 non-redundant proteins from the LB-enriched fraction. It is noteworthy that 91% of the proteins were identified by two peptides hits or more.

Classification of the Identified Proteins—The identified proteins were manually analyzed according to their cellular locations (Fig. 2*c*). Only a few proteins corresponded to endosomes (0.4%), melanosomes (0.2%), and peroxisomes (0.6%). The major classes corresponded to cytoplasmic (18.6%) and membrane (16.0%) proteins in accordance with the location of LBs in the cytoplasm of keratinocytes and with the fact that LBs are surrounded by a membrane. Other classes mainly represented include cytoskeleton (12.4%), nucleus (10.7%), and ribosomes (10.1%). When we tentatively classified the proteins in terms of relative abundance, as estimated by the number of MS/MS queries, we once again observed at the top of the list many cytoskeleton and ribosomal components. Even if this estimation was biased, *e.g.* hydrophobic proteins may be under-represented because of their biochemical properties, it shows the difficulty to obtain purified LBs and was clearly not sufficient to designate genuine constituents of LBs from possible contaminations. One possibility could be to quantitatively compare the distribution of the identified proteins all along the density gradient used to prepare the LB-enriched fraction using the protein correlation profiling approach (33). However, this approach in our case may be not completely differential: indeed if cytosoluble proteins are entrapped inside small size vesicles co-migrating with LBs during their enrichment (see "Discussion" for reasons of that) the contaminating proteins may not have a fractionation profile very different from that of true LB proteins. We also could test for the cellular localization of the identified proteins by immunohistology performed on skin sections with specific antibodies when available; a punctate labeling of the upper epidermal cells is suggestive of LB components. However, this is difficult to envisage with such a high number of proteins. We therefore chose a candidate approach based on the location and functional classification of the identified proteins with the help of both the literature knowledge and Ingenuity software. Some (331 of 984) turned out to be of particular interest (Table II and see Fig. 8) because of their potential role in desquamation and stratum corneum barrier function, *i.e.* the proteases (14 of 331), protease inhibitors (12 of 331), and secreted proteins (34 of 331). Confirming the close relationship between LBs and lysosomes, one of the major classes was lysosomal proteins (30 of 331). In connection with the involvement of calcium in the regulation of LB secretion, calcium-binding proteins (18 of 331) were observed. Among the 141 most interesting membrane proteins, some may be involved in the secretory mechanisms of LBs, such as the Rab proteins (19 of 331), Rab-associated proteins (10 of 331), and others proteins involved in all steps of vesicular trafficking and membrane fusion (38 of 331). Suggesting that LBs are transported along microtubules, components (27 of 331) of this class of cytoskeleton fibers were identified. Other classes represented include annexins (10 of 331); ion pumps, transporters, and channels (19 of 331); receptors (13 of 331); and signal transduction (55 of 331).

CLIP-170, a Protein Known to Mediate Interactions between Vesicles and Microtubules, and Its Direct Effector Cdc42 Are Associated with LBs Together with the Rab7 Protein—Among the proteins known to take part in vesicular and membrane trafficking, several direct and indirect effectors of a protein called CLIP-170/restin were highlighted using the Ingenuity software (Fig. 3). CLIP-170 is one of the cytoplasmic linker proteins, a class of proteins that facilitate the interaction between cellular organelles and microtubules. Because CLIP-170 itself was not present in the protein list obtained from nano-LC-MS/MS analysis, we went back to the Mascot database search results. CLIP-170 had indeed been identified but with a Mascot score too low to be validated. To confirm the presence of CLIP-170 in the LB-enriched fraction we immunodetected the protein sample with a monoclonal anti-CLIP-170 antibody specific for amino acids 1128–1427 (clone F3). As expected, a 170-kDa protein was specifically detected (Fig. 4). In IIF confocal microscopy analysis on skin cryosections (Fig 5*a*), the anti-CLIP-170 antibody displayed a punctate labeling, starting in the upper spinous keratinocytes at the nucleus periphery, and more intense labeling in the cytoplasm

TABLE II

List of the 331 more relevant proteins identified from the LB-enriched fraction

GM2, GalNAcβ4(Neu5Acα3)Galβ4Glc-ceramide; $GABA_A$, γ-aminobutyric acid, type A; DMPK, dystrophia myotonica protein kinase; SH3, Src homology 3; PLAUR, urokinase plasminogen activator surface receptor; CNDP, cytosolic non-specific dipeptidase; HLA, human leukocyte antigen.

Accession number	Gene name	Protein identified	Peptides matched; SC[a]
Proteases			
P13798	*APEH*	*N*-Acylaminoacyl-peptide hydrolase	11; 12%
Q13867	*BLMH*	Bleomycin hydrolase	9; 20%
P07384	*CAPN1*	Calpain 1, (μ/I) large subunit	33; 50%
P04632	*CAPNS1*	Calpain, small subunit 1	10; 53%
Q96L46	*CAPNS2*	Calpain, small subunit 2	10; 44%
Q96KP4	*CNDP2*	CNDP dipeptidase 2 (metallopeptidase M20 family)	7; 18%
Q5TDH0	*DDI2*	DNA damage-inducible 1, homolog 2	1; 4%
Q53SB6	*DNPEP*	Aspartyl aminopeptidase	1; 2%
P14735	*IDE*	Insulin-degrading enzyme	5; 6%
P55786	*NPEPPS*	Aminopeptidase puromycin-sensitive	12; 15%
Q9Y5X6	*PGCP*	Plasma glutamate carboxypeptidase	2; 5%
P12955	*PEPD*	Peptidase D	2; 2%
Q8N5P2	*SASP*	Saspase	1; 4%
P45974	*USP5*	Ubiquitin-specific peptidase 5 (isopeptidase T)	4; 7%
Protease inhibitors			
P20810	*CAST*	Calpastatin	5; 9%
P01040	*CSTA*	Cystatin A (stefin A)	6; 60%
P04080	*CSTB*	Cystatin B (stefin B)	2; 24%
P57730	*ICEBERG*	Caspase-1 inhibitor Iceberg	1; 10%
P01009	*SERPINA1*	Serpin peptidase inhibitor, clade A, member 1	9; 20%
P01011	*SERPINA3*	Serpin peptidase inhibitor, clade A, member 3	1; 3%
Q8IW75	*SERPINA12*	Serpin peptidase inhibitor, clade A, member 12	1; 2%
P36952	*SERPINB5*	Serpin peptidase inhibitor, clade B, member 5	19; 45%
P01008	*SERPINC1*	Serpin peptidase inhibitor, clade, member 1	5; 12%
P36955	*SERPINF1*	Serpin peptidase inhibitor, clade F, member 1	4; 14%
Q59EI5	*SERPING1*	Serpin peptidase inhibitor, clade G, member 1	2; 7%
P50454	*SERPINH1*	Serpin peptidase inhibitor, clade H, member 1	1; 6%
Secreted proteins			
Extracellular matrix			
P21810	*BGN*	Biglycan precursor (bone/cartilage proteoglycan I) (PG-S1)	1; 3%
Q9UMD9	*COL17A1*	Collagen, type XVII, α1	1; 1%[b]
P07585	*DCN*	Decorin	3; 7%
O00515	*LAD1*	Ladinin 1	6; 15%
P51884	*LUM*	Lumican	6; 22%
P20774	*OGN*	Osteoglycin (osteoinductive factor, mimecan)	2; 9%
Q15063	*POSTN*	Periostin, osteoblast-specific factor	17; 30%
Others			
Q9UCK6	None	Aspartylglucosaminidase β1 subunit	1; 68%
P02647	*APOA1*[c]	Apolipoprotein A-I	22; 66%
P02652	APOA2[c]	Apolipoprotein A-II precursor (Apo-AII) (ApoA-II)	3; 22%
P06727	APOA4[c]	Apolipoprotein A-IV	1; 2%
Q4ZG63	APOB[c]	Apolipoprotein B (including Ag(x) antigen)	6; 2%[b]
P02749	APOH[c]	Apolipoprotein H (β_2-glycoprotein I)	7; 28%
Q9NZ08	ARTS-1	Type 1 tumor necrosis factor receptor shedding aminopeptidase regulator	6; 8%
P25311	*AZGP1*	α_2-Glycoprotein 1, zinc	6; 27%
P61769	*B2M*	β_2-Microglobulin	10; 26%
P05452	*CLEC3B*	C-type lectin domain family 3, member B	1; 6%
O75629	*CREG1*	Cellular repressor of E1A-stimulated genes 1	4; 15%
P81605	*DCD*	Dermcidin	1; 10%
Q6E0U4	*DMKN*	Dermokine β	5; 13%
P02774	*GC*	Group-specific component (vitamin D-binding protein)	2; 6%
P18510	*IL1RN*	Interleukin 1 receptor antagonist	4; 20%
P09382	*LGALS1*	Lectin, galactoside-binding, soluble, 1 (galectin 1)	9; 59%
P17931	*LGALS3*	Lectin, galactoside-binding, soluble, 3 (galectin 3)	42; 44%
Q6IB87	*LGALS7*	Lectin, galactoside-binding, soluble, 7 (galectin 7)	262; 88%

TABLE II—*continued*

Accession number	Gene name	Protein identified	Peptides matched; SC[a]
P02788	*LTF*	Lactotransferrin precursor (lactoferrin)	3; 3%
P61626	*LYZ*	Lysozyme C (EC 3.2.1.17) (1,4-β-*N*-acetylmuramidase C)	1; 6%
P14174	*MIF*	Macrophage migration-inhibitory factor (glycosylation-inhibiting factor)	2; 17%
P30086	*PEBP1*	Phosphatidylethanolamine-binding protein 1	12; 76%
Q9H1E1	*RNASE7*	Ribonuclease, RNase A family, 7	5; 35%
Q6UWP8	*SBSN*	Suprabasin	9; 41%
Q6FH30	*SFN*	Stratifin	72; 83%
P08294	*SOD3*	Superoxide dismutase 3, extracellular	3; 15%
P02766	*TTR*	Transthyretin (prealbumin, amyloidosis type I)	5; 36%
Lysosomal proteins			
Q13510	*ASAH1*	*N*-Acylsphingosine amidohydrolase (acid ceramidase) 1	6; 19%
P38606	*ATP6V1A*	ATPase, H^+-transporting, lysosomal 70-kDa, V1 subunit A	14; 24%
P21281	*ATP6V1B2*	ATPase, H^+-transporting, lysosomal 56/58-kDa, V1 subunit B2	12; 29%
Q9Y5K8	*ATP6V1D*	ATPase, H^+-transporting, lysosomal 34-kDa, V1 subunit D	6; 39%
P36543	*ATP6V1E1*	ATPase, H^+-transporting, lysosomal 31-kDa, V1 subunit E1	7; 30%
Q16864	*ATP6V1F*	Vacuolar ATP synthase subunit F (EC 3.6.3.14)	3; 24%
O75348	*ATP6V1G1*	ATPase, H^+-transporting, lysosomal 13-kDa, V1 subunit G1	2; 17%[b]
Q9UI12	*ATP6V1H*	ATPase, H^+-transporting, lysosomal 50/57-kDa, V1 subunit H	5; 14%
Q9H3G5	*CPVL*	Probable serine carboxypeptidase CPVL precursor	13; 28%
P07339	*CTSD*	Cathepsin D (lysosomal aspartyl peptidase)	27; 10%
Q9UHL4	*DPP2*	Dipeptidyl-peptidase II	6; 11%
P04066	*FUCA1*	Fucosidase, α-L-1, tissue	5; 11%
P10253	*GAA*	Glucosidase, α; acid	2; 3%
P54803	*GALC*	Galactosylceramidase	1; 2%
P04062	*GBA*	Glucosidase, β; acid (includes glucosylceramidase)	2; 4%
Q92820	*GGH*	γ-Glutamyl hydrolase	3; 8%
P16278	*GLB1*	Galactosidase, β1	6; 11%
P17900	*GM2A*	GM2 ganglioside activator	6; 31%
P08236	*GUSB*	Glucuronidase, β	4; 6%
P07686	*HEXB*	Hexosaminidase B (βpolypeptide)	7; 16%
P11279	*LAMP1*	Lysosome-associated membrane protein 1	5; 14%
P13473	*LAMP2*	Lysosome-associated membrane protein 2	3; 7%
O00754	*MAN2B1*	Mannosidase, α, class 2B, member 1	2; 3%
P50897	*PPT1*	Palmitoyl-protein thioesterase 1	2; 9%[b]
P42785	*PRCP*	Prolyl carboxypeptidase (angiotensinase C)	3; 7%
P07602	*PSAP*	Prosaposin	3; 5%
Q14108	*SCARB2/ LIMP II*	Scavenger receptor class B, member 2	14; 31%
P51688	*SGSH*	*N*-Sulfoglucosamine sulfohydrolase (sulfamidase)	2; 3%
Q86T03	*TMEM55B*	Transmembrane protein 55B	1; 4%
O14773	*TPP1*	Tripeptidyl-peptidase I	6; 17%
Calcium-binding proteins			
S100 proteins			
Q3KRB9	*S100A2*	S100 calcium-binding protein A2	4; 22%
P26447	*S100A4*	S100 calcium-binding protein A4	6; 37%
Q5RHS4	*S100A6*	S100 calcium-binding protein A6 (calcyclin)	3; 24%
P05109	*S100A8*	S100 calcium-binding protein A8 (calgranulin A)	6; 53%
Q5T1C5	*S100A10*	S100 calcium-binding protein A10	15; 74%
P31949	*S100A11*	S100 calcium-binding protein A11 (calgizzarin)	6; 50%
Q9HCY8	*S100A14*	S100 calcium-binding protein A14	17; 71%
Q5RHS6	*S100A16*	S100 calcium-binding protein A16	9; 50%
Q9UDP3	None	Putative S100 calcium-binding protein H_NH0456N16.1	7; 33%
Others			
Q7Z4X0	*CAB39*	Calcium-binding protein 39	2; 5%[b]
P62158	*CALM*[c]	Calmodulin	19; 74%
P27482	CALML3	Calmodulin-like 3	9; 62%
Q9NZT1	*CALML5*	Calmodulin-like 5	5; 42%
P27797	*CALR*	Calreticulin	7; 20%
Q96C19	*EFHD2*	EF-hand domain family, member D2	7; 24%

TABLE II—*continued*

Accession number	Gene name	Protein identified	Peptides matched; SC[a]
Q9NZN4	*EHD2*[c]	EH-domain-containing 2	5; 14%
P84074	HPCA	Hippocalcin	2; 8%
P62760	*VSNL1*	Visinin-like 1	4; 22%
Membrane proteins			
Rab proteins			
P62820	*RAB1A*	RAB1A, member RAS oncogene family	19; 67%
Q9H1C9	*RAB1B*	RAB1B, member RAS oncogene family	4; 18%[b]
P61019	*RAB2*	RAB2, member RAS oncogene family	8; 44%
O95716	*RAB3D*	RAB3D, member RAS oncogene family	7; 32%
P20339	*RAB5A*	Ras-related protein Rab-5A	6; 29%
P61020	*RAB5B*	RAB5B, member RAS oncogene family	9; 47%
P51148	*RAB5C*	RAB5C, member RAS oncogene family	3; 19%
Q5U0A8	*RAB6A*	RAB6A, member RAS oncogene family	5; 21%
P51149	*RAB7*	RAB7, member RAS oncogene family	12; 59%
Q6FHV5	*RAB8A*	RAB8A, member RAS oncogene family	9; 31%
Q5JPC4	*RAB8B*	RAB8B, member RAS oncogene family	8; 24%
P61026	*RAB10*	RAB10, member RAS oncogene family	13; 35%
Q2YDT2	*RAB11B*	RAB11B, member RAS oncogene family	10; 48%
Q5U0A6	*RAB13*	RAB13, member RAS oncogene family	3; 12%
Q5JVD4	*RAB14*	RAB14, member RAS oncogene family	8; 45%
P59190	*RAB15*	RAB15, member RAS oncogene family	2; 10%
Q9UL25	*RAB21*	RAB21, member RAS oncogene family	6; 31%
O00194	*RAB27B*	RAB27B, member RAS oncogene family	1; 5%[b]
Q15286	*RAB35*	RAB35, member RAS oncogene family (RAB1C)	9; 24%
Rab-associated proteins			
Q07960	*ARHGAP1*	Rho GTPase-activating protein 1	9; 26%
P52565	*ARHGDIA*	Rho GDP dissociation inhibitor (GDI) α	6; 27%
P52566	*ARHGDIB*	Rho GDP dissociation inhibitor (GDI) β	6; 22%
Q5JYX0	*CDC42*	Cell division cycle 42 (GTP-binding protein, 25 kDa)	5; 40%[b]
P46940	*IQGAP1*	IQ motif-containing GTPase-activating protein 1	9; 13%
P49354	*FNTA*	Farnesyltransferase, C*AAX* box, α	2; 7%
P50395	*GDI2*	GDP dissociation inhibitor 2	22; 56%
P63000	*RAC1*[c]	Ras-related C3 botulinum toxin substrate 1 (Rac1)	6; 34%
P11233	RALA	v-ral simian leukemia viral oncogene homolog A	10; 44%
P112345	*RALB*	Ras-related protein Ral-B	9; 45%
Membrane trafficking			
Q10567	*AP1B1*	Adaptor-related protein complex 1, β1 subunit	12; 14%
O95782	*AP2A1*[c]	Adaptor-related protein complex 2, α1 subunit	9; 11%
P63010	AP2B1	Adaptor-related protein complex 2, β1 subunit	18; 21%
Q96CW1	*AP2M1*	Adaptor-related protein complex 2, μ1 subunit	13; 26%
P84077	*ARF1*	ADP-ribosylation factor 1	15; 64%
P18085	*ARF4*	ADP-ribosylation factor 4	8; 37%
P84085	*ARF5*	ADP-ribosylation factor 5	11; 44%
Q5U025	*ARF6*	ADP-ribosylation factor 6	5; 34%
P48444	*ARCN1*	Archain 1	5; 10%
Q96BM9	*ARL8A*	ADP-ribosylation factor-like 8A (10B)	4; 23%
Q96FZ7	*CHMP6*	Chromatin-modifying protein 6 (Vps20)	3; 11%
P53618	*COPB1*	Coatomer protein complex, subunit β1	3; 3%
P35606	*COPB2*	Coatomer protein complex, subunit β2 (β')	4; 6%
O14579	*COPE*	Coatomer protein complex, subunit ϵ	6; 30%
Q8WUI6	*COPG*	Coatomer protein complex, subunit γ	2; 4%
P61923	*COPZ1*	Coatomer protein complex, subunit ζ1	2; 17%
O75131	*CPNE3*	Copine III	7; 16%
O94832	*MYO1D*	Myosin-Id	3; 3%
Q9UFN0	*NIPSNAP3A*	nipsnap homolog 3A (*Caenorhabditis elegans*)	5; 30%
Q9BTU6	*PI4KII*	Phosphatidylinositol 4-kinase type II	1; 2%
Q9UL45	*PLDN*	Pallidin homolog (mouse)	2; 24
P62745	*RHOB*	ras homolog gene family, member B	3; 27%
O15127	*SCAMP2*	Secretory carrier membrane protein 2	2; 10%
Q15436	*SEC23A*	Sec23 homolog A (*Saccharomyces cerevisiae*)	2; 4%
Q15019	*SEPT2*	Septin 2	8; 23%

TABLE II—*continued*

Accession number	Gene name	Protein identified	Peptides matched; SC[a]
Q9UHD8	*SEPT9*	Septin 9	13; 23%
O00161	*SNAP23*	Synaptosome-associated protein, 23 kDa	5; 30%
P54920	*SNAPA*	α-Soluble NSF attachment protein (SNAP-α)	2; 9%[b]
Q13596	*SNX1*	Sorting nexin-1	5; 11%
O60749	*SNX2*	Sorting nexin-2	5; 10%
O60493	*SNX3*	Sorting nexin-3	4; 23%
Q6P5V6	*SNX5*	Sorting nexin-5	3; 8%[b]
Q9UNH7	*SNX6*	Sorting nexin-6	4; 9%
Q6FGP3	*TPD52*	Tumor protein D52	8; 55%
Q12846	*STX4*	Syntaxin 4	3; 10%
O43760	*SYNGR2*	Synaptogyrin 2	3; 12%
Q96QK1	*VPS35*	Vacuolar protein sorting 35	21; 30%
Q9BV40	*VAMP8*	Vesicle-associated membrane protein 8 (VAMP-8)	2; 18%
Annexins			
P04083	*ANXA1*	Annexin A1	25; 63%
Q8TBV2	*ANXA2*	Annexin A2	20; 58%
P12429	*ANXA3*	Annexin A3	6; 21%
P09525	*ANXA4*	Annexin A4	36; 68%
P08758	*ANXA5*	Annexin A5	58; 75%
P08133	*ANXA6*	Annexin A6	41; 61%
Q5T0M6	*ANXA7*	Annexin A7	6; 13%
Q5VTM4	*ANXA8*	Annexin A8	16; 53%
Q5VT79	*ANXA8L2*	Annexin A8-like 2	14; 50%
Q5T0G8	*ANXA11*	Annexin A11	12; 26%
Ion pumps, transporters, and channels			
P05023	*ATP1A1*[c]	ATPase, Na^+/K^+-transporting, α1 polypeptide	52; 41%
Q13733	ATP1A4	ATPase, Na^+/K^+-transporting, α4 polypeptide	2; 3%[b]
P54709	*ATP1B3*	ATPase, Na^+/K^+-transporting, β3 polypeptide	9; 30%
P16615	*ATP2A2*[c]	ATPase, Ca^{2+}-transporting, cardiac muscle, slow twitch 2	3; 5%[b]
P20020	ATP2B1	ATPase, Ca^{2+}-transporting, plasma membrane 1	9; 9%
P23634	*ATP2B4*	ATPase, Ca^{2+}-transporting, plasma membrane 4	8; 8%
O00299	*CLIC1*	Chloride intracellular channel 1	7; 39%
Q6UX81	*CLCA4*	Chloride channel, calcium-activated, family member 4	4; 6%
Q6KC16	*CYBRD1*	Cytochrome *b* reductase 1	1; 9%
P43003	*SLC1A3*	Solute carrier family 1, member 3	1; 2%
P43007	*SLC1A4*	Solute carrier family 1, member 4	3; 5%
Q15758	*SLC1A5*	Solute carrier family 1, member 5	1; 2%
P11166	*SLC2A1*	Solute carrier family 2 (facilitated glucose transporter), member 1	4; 8%
P08195	*SLC3A2*	Solute carrier family 3, member 2	4; 11%
P02730	*SLC4A1*	Solute carrier family 4, anion exchanger, member 1	22; 18%
Q00325	*SLC25A3*	Solute carrier family 25, member 3	4; 9%
Q02978	*SLC25A11*	Solute carrier family 25, member 11	6; 23%
P21796	*VDAC1*	Voltage-dependent anion channel 1	7; 29%
P45880	*VDAC2*	Voltage-dependent anion channel 2	5; 16%
Receptors			
P06126	*CD1A*	CD1a molecule	5; 11%
Q9H5A5	*CD44*	CD44 molecule (Indian blood group)	14; 11%
P78310	*CXADR*	Coxsackie virus and adenovirus receptor	7; 25%
P00533	*EGFR*[c]	Epidermal growth factor receptor	2; 2%
Q4QZC0	HLA-A	Major histocompatibility complex, class I, A	11; 41%
P30504	*HLA-Cw*4*	HLA class I histocompatibility antigen, Cw-4 α chain precursor	6; 17%[b]
P30685	*HLA-B*35*	HLA class I histocompatibility antigen, B-35 α chain precursor	10; 37%
P20039	*HLA-DRB5*	Major histocompatibility complex, class II, DRβ5	2; 6%[b]
P01903	*HLA-DRA*	Major histocompatibility complex, class II, DRα	10; 39%
Q5JPJ9	*LYPD3*	LY6/PLAUR domain-containing 3	6; 22%
O60664	*M6PRBP1*	Mannose 6-phosphate receptor-binding protein 1	14; 52%

TABLE II—*continued*

Accession number	Gene name	Protein identified	Peptides matched; SC[a]
O15031	*PLXNB2*	Plexin B2	8; 4%
P31431	*SDC4*	Syndecan 4 (amphiglycan, ryudocan)	1; 7%
Others			
Q59FP2	*ANK1*	Ankyrin 1, erythrocytic	6; 3%
P80723	*BASP1*	Brain-abundant, membrane-attached signal protein 1	6; 38%
O43570	*CA12*	Carbonic anhydrase XII	2; 11%
Q03135	*CAV1*[c]	Caveolin-1, caveolae protein, 22 kDa	9; 44%
Q5J7W6	CD9	CD9 molecule	4; 7%
Q6FHM9	*CD59*	CD59 molecule, complement-regulatory protein	3; 23%
Q5U0J6	*CD81*	CD81 molecule	3; 19%
Q6FG59	*CDC37*	CDC37 cell division cycle 37 homolog (*S. cerevisiae*)	5; 16%
Q5SYA8	*CD109*	CD109 molecule	36; 26%[b]
Q9UJ71	*CD207*	CD207 molecule, langerin	30; 61%
Q4KKX0	*EPB42*	Transglutaminase	11; 17%
Q9NZM1	*FER1L3*	fer-1-like 3, myoferlin	9; 6%
O75955	*FLOT1*[c]	Flotillin 1	5; 12%
Q14254	FLOT2[c]	Flotillin 2	6; 17%
Q9HCC8	GDPD2	Glycerophosphodiester phosphodiesterase domain-containing 2	2; 6%
Q9NZD2	*GLTP*	Glycolipid transfer protein	3; 16%
P35052	*GPC1*	Glypican 1	4; 11%
Q14956	*GPNMB*	Glycoprotein (transmembrane) nmb	5; 5%
O43813	*LANCL1*	LanC lantibiotic synthetase component C-like 1 stomatin-interacting	16; 39%
Q92597	*NDRG1*	N-myc downstream regulated gene 1	14; 40%
P01111	*NRAS*	Neuroblastoma RAS viral (v-ras) oncogene homolog	2; 13%[b]
Q9NP74	*PALMD*	Palmdelphin	9; 5%
Q04941	*PLP2*	Proteolipid protein 2 (colonic epithelium-enriched)	1; 9%
Q6NZI2	*PTRF*	Polymerase I and transcript release factor	10; 19%
P07237	*P4HB*	Procollagen-proline, 2-oxoglutarate 4-dioxygenase	25; 49%
P61225	*RAP2B*	RAP2B, member of RAS oncogene family	6; 41%
P61586	*RHOA*[c]	ras homolog gene family, member A	12; 48%
P40967	SILV	Silver homolog (mouse)	7; 3%
P27105	*STOM*	Stomatin	15; 56%
Q7Z7Q4	*TACSTD2*	Tumor-associated calcium signal transducer 2	11; 30%
Q14134	*TRIM29*	Tripartite motif-containing 29	18; 29%
Q99536	*VAT1*	Vesicle amine transport protein 1 homolog (*Torpedo californica*)	18; 44%
Microtubules			
Tubulins			
P68363	*K-ALPHA-1*	α-Tubulin	28; 49%
P68366	*TUBA1*	Tubulin, α1	29; 53%
Q71U36	*TUBA3*	Tubulin, α3	20; 53%
Q9BQE3	*TUBA6*	Tubulin, α6	28; 49%
P07437	*TUBB*	Tubulin, β	29; 70%
Q6FGZ8	*TUBB2A*	Tubulin, β2A	1; 4%
P68371	*TUBB2C*	Tubulin, β2C	43; 70%
Q3ZCR3	*TUBB3*	Tubulin, β3	1; 6%
Q969E5	*TUBB4*	Tubulin, β4	35; 63%
Q4QQJ5	*TUBAL3*	Tubulin, α-like 3	4; 8%
Microtubule-associated proteins			
Q9NVJ2	*ARL8B*	ADP-ribosylation factor-like 8B	6; 33%
Q13561	*DCTN2*	Dynactin 2 (p50)	7; 22%
Q16555	*DPYSL2*	Dihydropyrimidinase-like 2	9; 19%
Q14204	*DYNC1H1*	Dynein, cytoplasmic 1, heavy chain 1	20; 6%
Q13409	*DYNC1I2*	Dynein, cytoplasmic 1, intermediate chain 2	13; 21%
P63167	*DYNLL1*	Dynein, light chain, LC8-type 1	6; 51%
Q9NP97	*DYNLRB1*	Dynein, light chain, roadblock-type 1	2; 12%
P63172	*DYNLT1*	Dynein, light chain, Tctex-type 1	1; 16%
Q59EN8	*EML2*	Echinoderm microtubule-associated protein-like 2	5; 8%

TABLE II—*continued*

Accession number	Gene name	Protein identified	Peptides matched; SC[a]
Q4L233	*FREP1*	Similar to tubulin polymerization-promoting protein (TPPP)	3; 11%
O95166	*GABARAP*	$GABA_A$ receptor-associated protein	2; 12%
Q9H2C0	*GAN*	Giant axonal neuropathy (gigaxonin)	15; 30%
Q07866	*KNS2*	Kinesin 2	1; 2%
Q86UP2	*KTN1*	Kinectin 1 (kinesin receptor)	10; 10%[b]
P27816	*MAP4*	Microtubule-associated protein 4	10; 8%
P43034	*PAFAH1B1*	Platelet-activating factor acetylhydrolase, isoform Ib	18; 43%
P16949	*STMN1*	Stathmin 1/oncoprotein 18	5; 35%
Signal transduction			
Q9UQB8	*BAIAP2*	BAI1-associated protein 2	7; 12%
Q5VT25	*CDC42BPA*	CDC42-binding protein kinase α (DMPK-like)	2; 1%
P48729	*CSNK1A1*	casein kinase 1, α1	12; 29%
P61201	*COPS2*	COP9 constitutive photomorphogenic homolog subunit 2	4; 10%
Q59GH5	*COPS5*	COP9 constitutive photomorphogenic homolog subunit 5	3; 13%
Q9UBW8	*COPS7A*	COP9 constitutive photomorphogenic homolog subunit 7A	1; 6%
P07108	*DBI*	Acyl-CoA-binding protein (ACBP) (diazepam-binding inhibitor) (DBI)	6; 63%
Q6FI36	*DUSP14*	Dual specificity phosphatase 14	3; 18%
P29992	*GNA11*	Guanine nucleotide-binding protein (G protein), α-11 (G_q class)	10; 30%
Q14344	*GNA13*	Guanine nucleotide-binding protein α-13 subunit (Gα-13)	5; 10%
P63096	*GNAI1*	Guanine nucleotide-binding protein, α-inhibiting activity polypeptide 1	22; 55%
Q6B6N3	*GNAI2*[c]	Guanine nucleotide-binding protein, α-inhibiting activity polypeptide 2	29; 50%
P08754	GNAI3	Guanine nucleotide-binding protein, α-inhibiting activity polypeptide 3	20; 57%
P38405	*GNAL*	Guanine nucleotide-binding protein, α-activating activity polypeptide	3; 6%
P50148	*GNAQ*[c]	Guanine nucleotide-binding protein (G protein), q polypeptide	8; 24%
P63092	GNAS	GNAS complex locus	8; 16%
P11488	*GNAT1*	Guanine nucleotide-binding protein G_t, α-1 subunit	2; 5%[b]
P62873	*GNB1*	Guanine nucleotide-binding protein, β polypeptide 1	14; 49%
P63244	*GNB2L1*	Guanine nucleotide-binding protein, β polypeptide 2-like 1	11; 33%
P63218	*GNG5*	Guanine nucleotide-binding protein γ-5 subunit precursor	3; 32%
Q9UBI6	*GNG12*	Guanine nucleotide-binding protein, γ-12	8; 75%
P62993	*GRB2*	Growth factor receptor-bound protein 2	10; 57%
P28482	*MAPK1*[c]	Mitogen-activated protein kinase 1	8; 19%
Q9UHA4	MAP2K1IP1	Mitogen-activated protein kinase kinase 1-interacting protein 1	3; 27%
Q14764	*MVP*	Major vault protein	19; 23%
Q92882	*OSTF1*	Osteoclast-stimulating factor 1	3; 21%
P68402	*PAFAH1B2*	Platelet-activating factor acetylhydrolase, isoform Ib, β subunit	4; 14%
Q6ZSH5	*PDIA6*	Highly similar to protein-disulfide isomerase A6	11; 37%
Q99623	*PHB2*	Prohibitin 2	4; 18%
Q01970	*PLCB3*	Phospholipase C, β3 (phosphatidylinositol-specific)	4; 5%[b]
P62136	*PPP1CA*	Protein phosphatase 1, catalytic subunit, α isoform	5; 22%
P62140	*PPP1CB*	Protein phosphatase 1, catalytic subunit, β isoform	4; 12%
P30153	*PPP2R1A*	Protein phosphatase 2 (formerly 2A), regulatory subunit A, α isoform	18; 32%
P63151	*PPP2R2A*	Protein phosphatase 2 (formerly 2A), regulatory subunit B, α isoform	7; 16%
Q08209	*PPP3CA*	Protein phosphatase 3 (formerly 2B), catalytic subunit, α isoform	9; 18%
P17612	*PRKACA*[c]	Protein kinase, cAMP-dependent, catalytic, α	4; 11%
P54619	PRKAG1	Protein kinase, AMP-activated, γ1 non-catalytic subunit	2; 6%
P13861	*PRKAR2A*[c]	Protein kinase, cAMP-dependent, regulatory, type II, α	13; 34%
Q969G5	PRKCDBP	Protein kinase C, δ -binding protein	4; 15%
Q99873	*PRMT1*	Protein-arginine *N*-methyltransferase	1; 3%
P08134	*RHOC*	ras homolog gene family, member C	9; 41%

TABLE II—*continued*

Accession number	Gene name	Protein identified	Peptides matched; SC[a]
Q7L523	*RRAGA*	Ras-related GTP-binding A	1; 5%
Q9H202	*RRAGC*	Ras-related GTP-binding protein C	4; 11%
P10301	*RRAS*	Related RAS viral (r-ras) oncogene homolog	5; 27%
Q9H299	*SH3BGRL3*	SH3 domain-binding glutamic acid-rich protein-like 3	5; 31%
Q9Y3L3	*SH3BP1*	SH3 domain-binding protein 1	6; 11%
Q5JV98	*STK24*	Serine/threonine kinase 24	3; 15%
Q9Y3F4	*STRAP*	Serine/threonine kinase receptor-associated protein	5; 15%
Q9Y6W5	*WASF2*	Wiskott-Aldrich syndrome protein family member 2	5; 13%
P31946	*YWHAB*	14-3-3 protein β/α	70; 72%
Q4VJB6	*YWHAE*	14-3-3 protein ϵ isoform transcript variant 1	38; 21%
P61981	*YWHAG*	14-3-3 protein γ	57; 55%
Q04917	*YWHAH*	14-3-3 protein η	54; 48%
P27348	*YWHAQ*	14-3-3 protein θ	52; 44%
Q32P43	*YWHAZ*	Tyrosine 3-/tryptophan 5-monooxygenase activation protein	98; 99%

[a] Sequence coverage. Except where noted, the sequence coverage and number of matched peptides correspond to the MS/MS analysis of the proteins separated on the longer gel (see supplemental Table 3).

[b] The sequence coverage and number of matched peptides correspond to the MS/MS analysis of the proteins identified in the analysis of the short (7-cm-long) gel fractionated into 16 slices.

[c] Proteins known to either interact with caveolin or be a component of caveolae.

of the granular keratinocytes. This pattern, which can be clearly observed in a reconstructed three-dimensional view (supplemental Fig. 3), was highly suggestive of the labeling of vesicles that could be LBs. Indeed the stained structures showed a diameter of 240 ± 120 nm (n = 1107), which is in accordance with the previously described size of LBs. Because CLIP-170 is considered as a ubiquitously expressed microtubule-binding protein, we were surprised of this labeling that was mainly restricted to the more differentiated keratinocytes. We therefore performed two types of control experiments. First, we tested the anti-CLIP-170 monoclonal antibody F3 on HeLa cells by double staining IIF using a polyclonal anti-tubulin antibody. As expected, we observed a patchy distribution in the interphase cells often organized into linear arrays that correlate with microtubules. Moreover there was an accumulation of CLIP-170 at the peripheral ends of some but not all microtubules (supplemental Fig. 4a). Second, we analyzed the expression of CLIP-170 in human epidermis by IIF using another unrelated antibody, namely N18, directed against the amino terminus of the protein. Once again, we only detected CLIP-170 in the upper part of the epidermis with a punctate labeling of the granular keratinocytes (supplemental Fig. 4b). We then performed double stainings of normal skin cryosections with the anti-CLIP-170 monoclonal antibody F3 and with polyclonal rabbit antibodies directed against either corneodesmosin or cathepsin D, two LB markers (Fig. 5, *b–d*). Corneodesmosin was mainly detected in the granular keratinocytes as published previously (34). CLIP-170 and corneodesmosin showed few co-locations, and only a few anti-CLIP-170-labeled vesicles were stained by the anti-corneodesmosin antibodies (9%, n = 110). Cathepsin D was detected in the cytoplasm of all keratinocytes with a more intense labeling of the granular cells as described previously (4). In the granular keratinocytes, a large proportion (88%, n = 124) of anti-CLIP-170-labeled vesicles were stained by the anti-cathepsin D antibodies (Fig. 5, *c* and *d*). These data suggest that CLIP-170 is associated with a subpopulation of LBs, at least those containing cathepsin D.

CLIP-170 is known to form a tripartite complex with IQ motif-containing GTPase-activating protein 1 (IQGAP1) and Rac1/Cdc42 (35). Because Rac1 is only expressed in the basal layer of human epidermis (36), we were interested in a possible interaction in the upper epidermis between CLIP-170 and Cdc42. Rab proteins have been reported to recruit effectors to specific membrane compartments in their GTP-bound form and are involved in vesicular trafficking (37, 38), and Rab11 has been shown to be associated with epidermal LB (25). In particular, Rab7 may regulate exocytosis of vesicles with endosomal/lysosomal characteristics, via the CLIP-170 tripartite complex, by binding Cdc42 (39). We therefore checked for a possible co-location of CLIP-170, IQGAP1, Cdc42, and Rab7 in the human epidermis.

First we confirmed the presence of both CLIP-170 partners (IQGAP1 (190 kDa) and Cdc42 (25 kDa)) and of Rab7 (23 kDa) in the LB-enriched fraction by Western blotting (Fig. 4). We then analyzed their expression on human normal skin cryosections by IIF and confocal microscopy (Fig. 6). IQGAP1 was detected in the cytoplasm of all keratinocytes with a more intense staining at the cell periphery as described previously (40). Anti-Cdc42 antibodies labeled the cytoplasm of keratinocytes in all layers of the epidermis with an increased staining intensity at the nucleus periphery. Double labeling did not reveal any particular co-location of CLIP-170 and IQGAP1 (Fig. 6*a*), whereas many anti-CLIP-170-labeled vesicles in the granular layer were also stained by the anti-Cdc42 antibodies (84%, n = 115) (Fig. 6, *b* and *d*). Confirming an interaction between CLIP-170 and Cdc42, we identified Cdc42 by MS as co-immunoprecipitated from

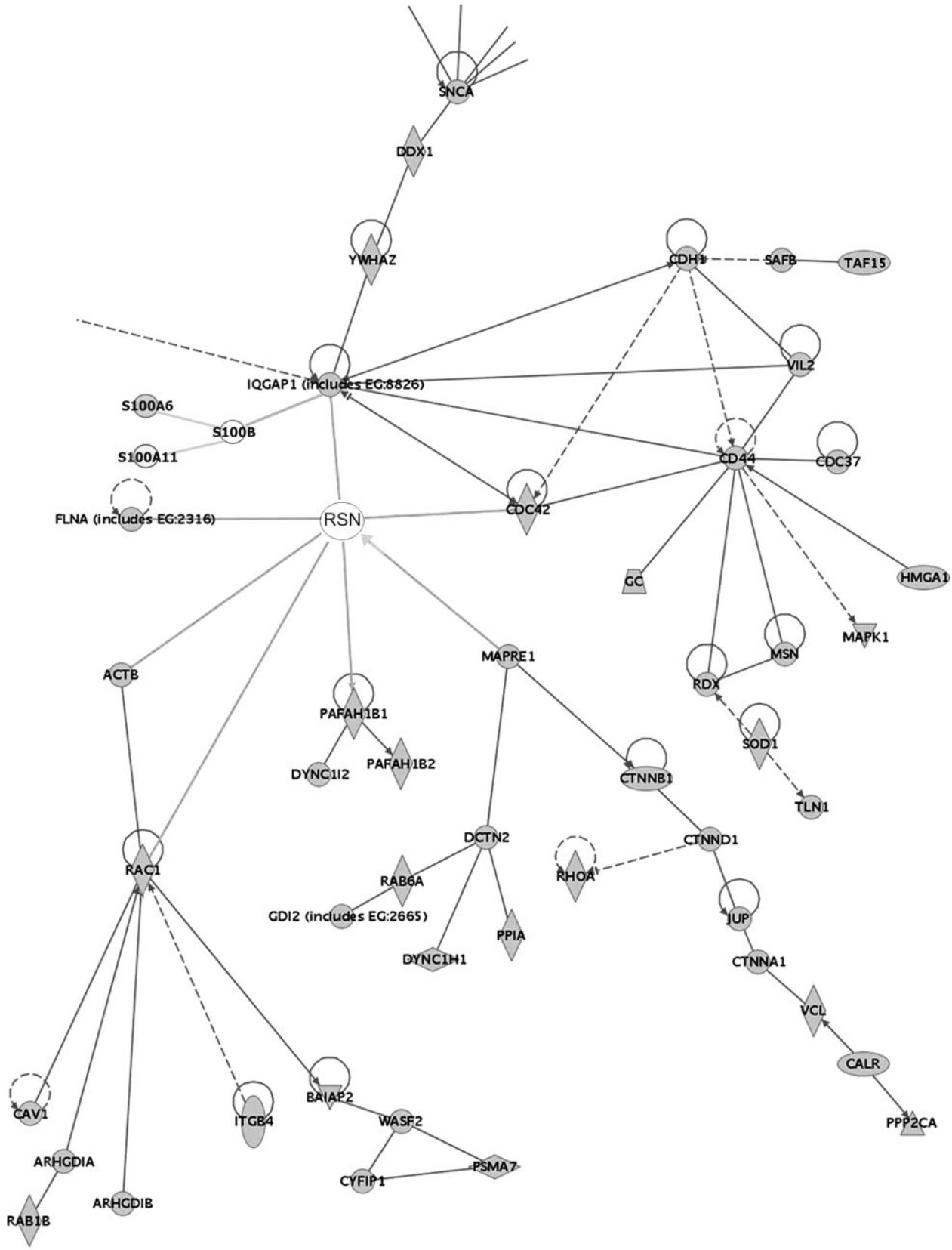
SNCA
DDX1
YWHAZ
CDH1
SAFB
TAF15
VIL2
IQGAP1 (includes EG:8826)
S100A6
S100B
S100A11
CD44
CDC37
FLNA (includes EG:2316)
RSN
CDC42
GC
HMGA1
MAPK1
MSN
RDX
SOD1
TLN1
ACTB
MAPRE1
PAFAH1B1
PAFAH1B2
DYNC1I2
CTNNB1
DCTN2
CTNND1
RAC1
RAB6A
RHOA
GDI2 (includes EG:2665)
PPIA
DYNC1H1
JUP
CTNNA1
VCL
CALR
PPP2CA
CAV1
ITGB4
BAIAP2
WASF2
ARHGDIA
CYFIP1
PSMA7
ARHGDIB
RAB1B

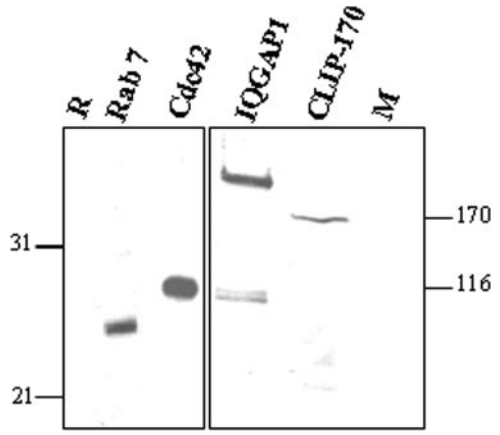

FIG. 4. **Immunodetection of Rab7, Cdc42, IQGAP1, and CLIP-170 in the LB-enriched fraction.** Proteins of the LB-enriched fraction were immunodetected with the anti-Rab7 and anti-Cdc42 rabbit polyclonal antibodies and with the anti-IQGAP1 and anti-CLIP-170 monoclonal antibodies as indicated. As controls, they were immunodetected only with the secondary antibodies directed against either rabbit (*R*) or mouse (*M*) immunoglobulins. The position of molecular mass standards is indicated in kDa.

an epidermal extract (Tris-EDTA-Nonidet P-40 extract) by the anti-CLIP-170 antibodies but not by an isotypic negative control (data not shown). Anti-Rab7 antibodies mainly produced a cytoplasmic labeling of the granular keratinocytes (Fig 6*c*). Some of the CLIP-170 and Rab7 were also shown to be co-localized; some vesicles (43%, $n = 101$) were labeled by both anti-CLIP-170 and anti-Rab7 antibodies (Fig. 6, *c* and *e*).

Furthermore we observed a partial co-localization between Rab7 and corneodesmosin (Fig. 7, *a* and *c*). There was a clear, puzzling co-localization between corneodesmosin and Cdc42 in the granular keratinocytes (Fig. 7, *b* and *d*). This suggests that Cdc42 is associated with most if not all LBs, including those containing corneodesmosin, but not routed via CLIP-170 molecules.

DISCUSSION

Efficacy and Limits of the Preparation of the LB-enriched Fraction

We modified and improved a previously described protocol for the preparation of an LB-enriched fraction from human epidermis; in particular, we added a filtration step that largely removed membrane sheets and melanosome contamination. The final fraction obtained was mainly composed of vesicles with morphology and size similar to that of LBs. The presence and/or enrichment of known LB markers (caveolin-1, kallikrein-7, kallikrein-8, corneodesmosin, and dermokine) was evidenced by Western blotting and immunoelectron microscopy, confirming the efficacy of the method. However, the organelles seemed to be partly emptied of their genuine cargos as shown by electron microscopy observations and by the fact that the enrichment of the membrane protein caveolin-1 was more effective than that of secreted proteins (kallikreins and corneodesmosin) (Fig. 1). This could be related to the tubulovesicular nature of LBs and to their proposed intertwining with cell cytoskeletons (2), which would induce their damage during cell fractionation. As expected, when we compared the proteins of the LB-enriched fraction identified by LC-MS/MS with the proteins of the S100 fraction, we noted a clear increase in the number of known membrane and membrane-associated proteins (16 *versus* 5%) (Fig. 2, *a* and *b*). Further confirming the efficiency of the fractionation, only a few of the 984 proteins identified corresponded to melanosome (2 of 984) or peroxisome (5 of 984) intrinsic components (Fig. 2*c*). The main contaminants of our preparation seemed to be nuclearly and cytoplasmically abundant proteins, in particular mitochondrial, ribosomal, and proteasomal compo-

Fig. 3. **Ingenuity pathway network obtained on a set of proteins identified in the LB-enriched fraction interacting directly or indirectly with CLIP-170.** Of the 984 proteins identified in the LB-enriched fraction uploaded into Ingenuity pathway analysis software, more than 50 are direct or indirect interaction partners of CLIP-170/restin (*RSN*). Proteins with a *gray background* were detected in the LB-enriched fraction, whereas proteins with a *clear background* were not. *ACTB*, actin β; *ARHGDIA*, Rho GDP dissociation inhibitor (GDI) α; *ARHGDIB*, Rho GDP dissociation inhibitor (GDI) β; *CALR*, calreticulin; *CAV1*, caveolin-1; *CD44*, CD44 molecule; *CDC37*, cell division cycle 37; *CDC42*, cell division cycle 42; *CDH1*, cadherin 1; *CTNNA1*, catenin α1; *CTNNB1*, catenin β1; *CTNND1*, catenin δ1; *CYFIP1*, cytoplasmic FMR1-interacting protein 1; *DCTN2*, dynactin 2; *DDX1*, DEAD (Asp-Glu-Ala-Asp) box polypeptide 1; *DYNC1H1*, dynein, cytoplasmic 1, heavy chain 1; *DYNC1I2*, dynein, cytoplasmic 1, intermediate chain 2; *FLNA*, filamin A; *GC*, group-specific component (vitamin D-binding protein); *GDI2*, GDP dissociation inhibitor 2; *HMGA1*, high mobility group AT-hook 1; *ITGB4*, integrin β4; *JUP*, junction plakoglobin; *MAPK1*, mitogen-activated protein kinase 1; *MAPRE1*, microtubule-associated protein RP/EB family, member 1; *MSN*, moesin; *PAFAH1B1*, platelet-activating factor acetylhydrolase, isoform Ib subunit 1; *PAFAH1B2*, platelet-activating factor acetylhydrolase, isoform Ib subunit 2; *PPIA*, peptidylprolyl isomerase A; *PPP2CA*, protein phosphatase 2 catalytic subunit, α isoform; *PSMA7*, proteasome subunit, α type, 7; *RAB1B*, RAB1B, member RAS oncogene family; *RAB6A*, RAB6A, member RAS oncogene family; *RAC1*, ras-related C3 botulinum toxin substrate 1; *RDX*, radixin; *RHOA*, ras homolog gene family, member A; *RSN*, CAP-GLY domain-containing linker protein 1; *S100A6*, S100 calcium-binding protein A6; *S100A11*, S100 calcium-binding protein A11; *S100B*, S100 calcium-binding protein B; *SAFB*, scaffold attachment factor B; *SNCA*, synuclein α; *SOD1*, superoxide dismutase 1; *TAF15*, TAF15 RNA polymerase II; *TLN1*, talin 1; *VCL*, vinculin; *VIL2*, villin 2; *WASF2*, WAS protein family, member 2; *YWHAZ*, tyrosine 3-monooxygenase/tryptophan 5-monooxygenase activation protein, ζ polypeptide. The major interactions found between these proteins are indicated by different *arrows*. *Solid thick line*, binding; *solid thick arrow*, acts on; *dashed thin line*, indirect interaction; *solid thin line*, direct interaction; *horizontally elongated diamond*, peptidase; *triangle*, phosphatase; *inverted triangle*, kinase; *vertically elongated diamond*, other enzyme; *trapezoid*, transporter; *horizontally elongated oval*, transcription regulator; *vertically elongated oval*, transmembrane receptor; *circle*, others.

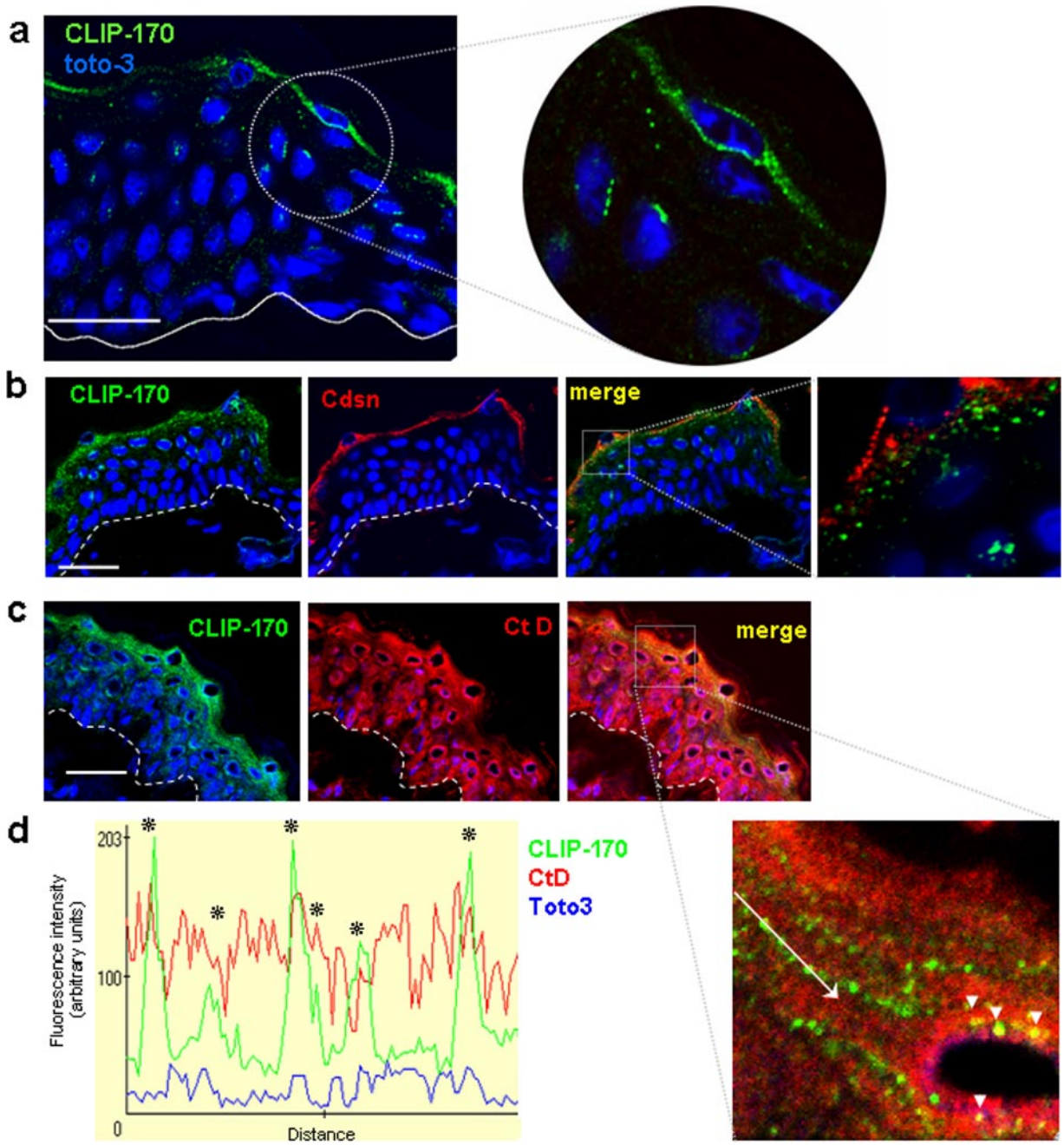

FIG. 5. **CLIP-170 is expressed in the differentiated epidermal keratinocytes and is partially co-localized with cathepsin D, a marker of LBs.** Normal human skin cryosections were analyzed by confocal laser microscopy using anti-CLIP-170 (*a*), anti-corneodesmosin (*Cdsn*) (*b*), and anti-cathepsin D (*CtD*) (*c*) antibodies. Nuclei (*blue*) are visualized with Toto-3. Image superpositions of CLIP-170/corneodesmosin and CLIP-170/cathepsin D are shown (*merge*). Co-locations are indicated by *white arrowheads*. In the presence of non-immune antibodies and in the absence of primary antibodies, no significant immunoreactivities were observed (data not shown). The *dotted lines* indicate the dermoepidermal junction. *Scale bars*, 75 μm; *enlargement*, $\times$7.5. *d*, the spectral profiles of each fluorochrome (Alexa Fluor 488 (*green*), Alexa Fluor 555 (*red*), and Toto-3 (*blue*)) detected on six different anti-CLIP-170-labeled vesicles (along the *white arrow* shown in the *enlargement* of *c*)) are shown. Co-localization of the *green* and *red* fluorochromes is indicated by *stars*.

nents and glycolytic enzymes. This could be due to the great abundance of these proteins in the cells and/or to their physicochemical properties, which cause them to interact with membranes after cell fractionation, as reported in a similar proteomics analysis strategy (41). Moreover during the enrichment procedure, high mechanical forces must be applied to disrupt the skin tissues and keratinocytes that may damage the cytoplasmic organelles. LBs may open and close up, encapsulating cytoplasmic proteins. Also other types of damaged organelles as well as pieces of plasma membrane can

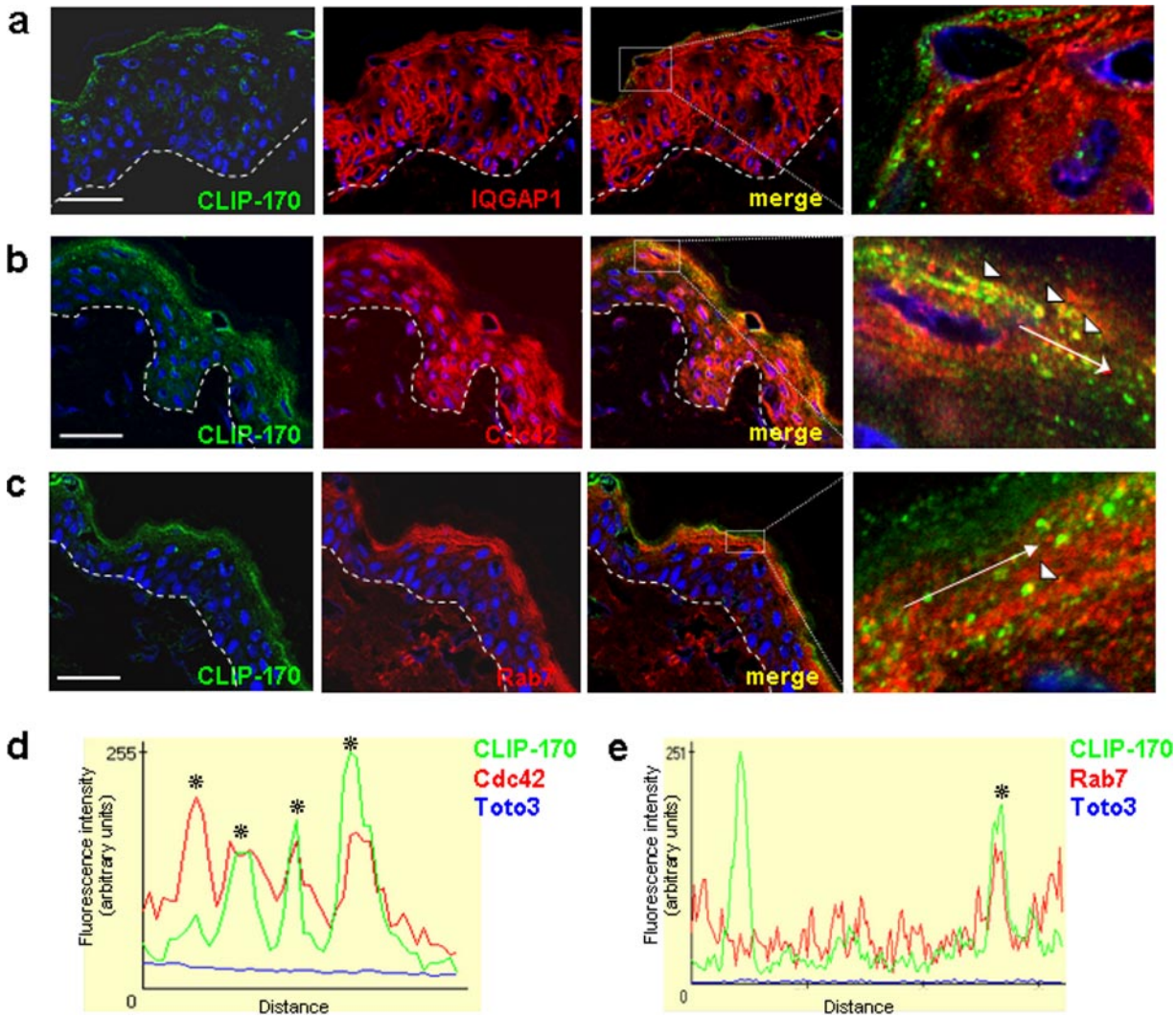

FIG. 6. **CLIP-170 expression in normal human epidermis overlaps with that of its previously described effector Cdc42 and of Rab7.** Normal human skin cryosections were analyzed by confocal laser microscopy using anti-CLIP-170 antibodies and anti-IQGAP1 (*a*), anti-Cdc42 (*b*), and anti-Rab7 (*c*) antibodies. Nuclei (*blue*) are visualized with Toto-3. Image superpositions of CLIP-170/IQGAP1, CLIP-170/Cdc42, and CLIP-170/Rab7 are shown (*merge*). Co-locations are indicated by *white arrowheads*. The *dotted lines* indicate the dermoepidermal junction. *Scale bars*, 75 μm; *enlargement*, $\times$7.5. *d* and *e*, the spectral profiles of each fluorochrome (Alexa Fluor 488 (*green*), Alexa Fluor 555 (*red*), and Toto-3 (*blue*)) detected on different anti-CLIP-170-labeled vesicles (along the *white arrows*) are shown. Co-localization of the *green* and *red* fluorochromes is indicated by *stars*.

close up in the same way and form small size vesicles full of cytoplasmically abundant proteins. They may subsequently co-migrate with LB vesicles on the density gradient, and their protein content would then be preferentially identified during the nano-LC-MS/MS analysis. Thus, it may be difficult to distinguish between genuine components of the LBs, proteins associated with the LB vesicles, or contaminating proteins. For example, many of the MS/MS-identified proteins in the LB-enriched fraction corresponded to actin (76 of 984) cytoskeleton. This could either be because these proteins are abundant in the cells or, more likely, because cytoskeleton elements become attached to the vesicles that pass along them. In the following sections, we discuss some proteins identified in this study that seem relevant in light of the known function of LBs. Moreover we chose a candidate approach to go further into the analysis of the present data and performed validation and functional experiments on some particular proteins to show their implication in the trafficking of LBs.

Analysis of the Epidermal LB Proteome

Overall 984 proteins were identified from the LB-enriched fraction. For most of them, this is the first evidence of their expression in human epidermis. Four hundred seventy-six have been shown to be expressed in the granular layer of the epidermis at the mRNA level (42).

Among the identified proteins, we found caveolin-1 and 21 proteins that have been previously localized in caveolae

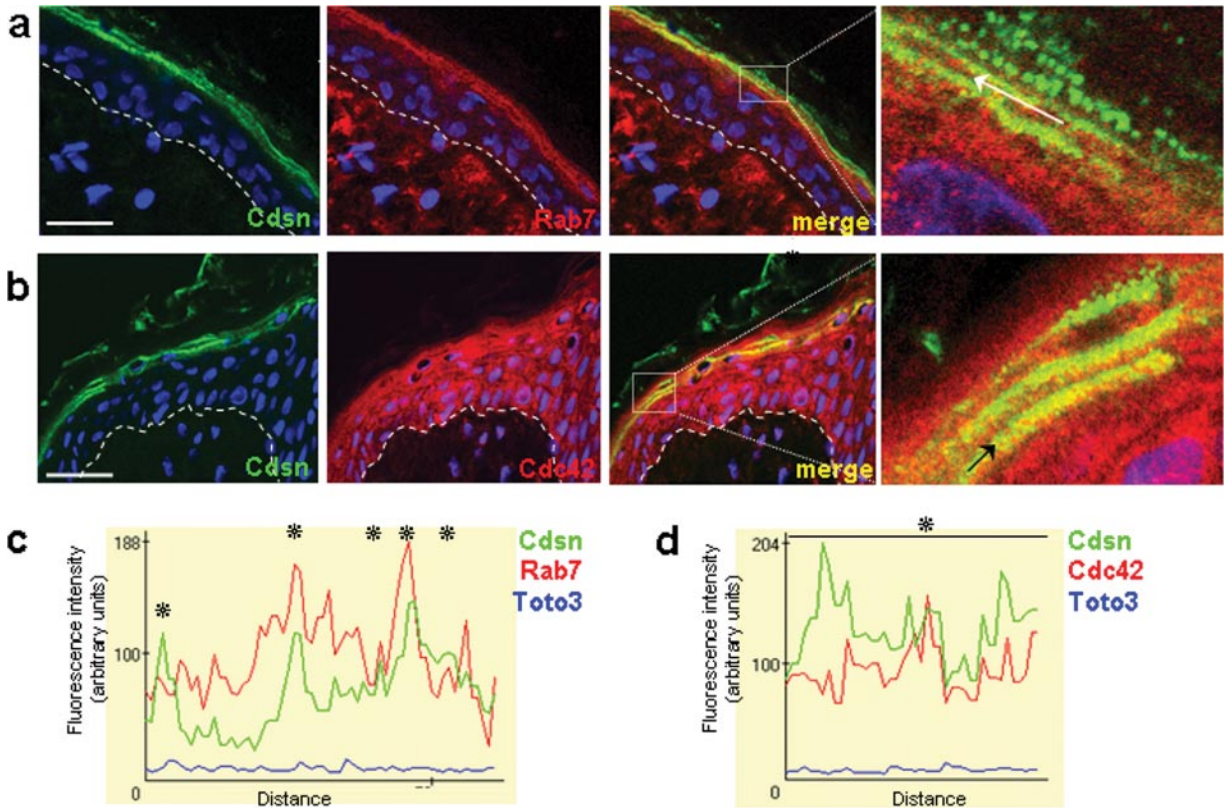

FIG. 7. **Comparison between corneodesmosin, Cdc-42, and Rab-7 location in normal human epidermis.** Normal human skin cryosections were analyzed by confocal laser microscopy using anti-corneodesmosin monoclonal antibody (*Cdsn*) and either anti-Rab7 (*a*) or anti-Cdc-42 (*b*) antibodies as indicated. Nuclei (*blue*) are visualized with Toto-3. Image superpositions of corneodesmosin/Cdc42 and corneodesmosin/Rab7 are shown (*merge*). Co-location is indicated by the *yellow* color. The *dotted lines* indicate the dermoepidermal junction. *Scale bars*, 75 μm; *enlargement*, $\times$7.5. *a* and *b*, the spectral profiles of each fluorochrome (Alexa Fluor 488 (*green*), Alexa Fluor 555 (*red*), and Toto-3 (*blue*)) detected on different anti-CLIP-170-labeled vesicles (along the *white* and *black arrows*) are shown. Co-localization of the *green* and *red* fluorochromes is indicated by *stars*.

and/or described to interact with caveolin-1 (Table II), confirming the suspected role of caveolae in the organization and/or function of LB (15). For example, apolipoproteins (A-I, A-II, A-IV, B, and H) may be involved in cholesterol and phospholipid transport in collaboration with ABCA receptors (43). Flotillins 1 and 2, considered as markers for lipid microdomains, have been reported to play a role in vesicle trafficking and cytoskeleton rearrangement (44, 45). Interestingly flotillin 1 has been localized in endo/lysosomal vesicles in adipocytes (46) and identified in fractions enriched in lysosomes of natural killer T cells (47, 48). Caveolae serve as assembly sites for signaling complexes (49), and we consistently identified 54 proteins known to play a role in signal transduction like kinases, phosphatases, and guanine nucleotide-binding proteins, including some already known to interact with caveolae: mitogen-activated protein kinase 1 and protein kinase A (50, 51). The way these proteins might influence epidermal LB secretion and more widely the role of caveolae proteins in LB remain to be discovered.

Based on the identification of proteins that are or may be either transported into LBs or involved in LB trafficking, we propose a functional model of these secretory structures (Fig. 8). It is discussed in detail below. Clearly more investigations are required to determine whether these proteins are really localized at the level of LBs and, for some of them, in the stratum corneum extracellular spaces and to dissect what role they play in the upper epidermis, *e.g.* immunoelectron microscopy analysis with specific antibodies, or small interfering RNA inactivation in three-dimensional skin models (necessary to achieve sufficient differentiation of cultured keratinocytes to get LBs).

Secreted Proteins—Among the 984 proteins, five are already known to be secreted via LBs: two proteases, cathepsin D and kallikrein 7 (the latter protein did not satisfy the criteria used for automatic validation but was identified with a total Mascot score of 54.85 and two top ranking peptides for which the MS/MS spectra were verified manually and are shown in supplemental Fig. 2); the β-glucosylceramidase involved in the maturation of glucosylceramides to ceramides in the stratum corneum; and two proteins with unknown function, dermokine β and suprabasin (52).

Five proteins have been previously reported to be expressed in the granular layer of the epidermis and present in the stratum corneum. They have been supposed to be com-

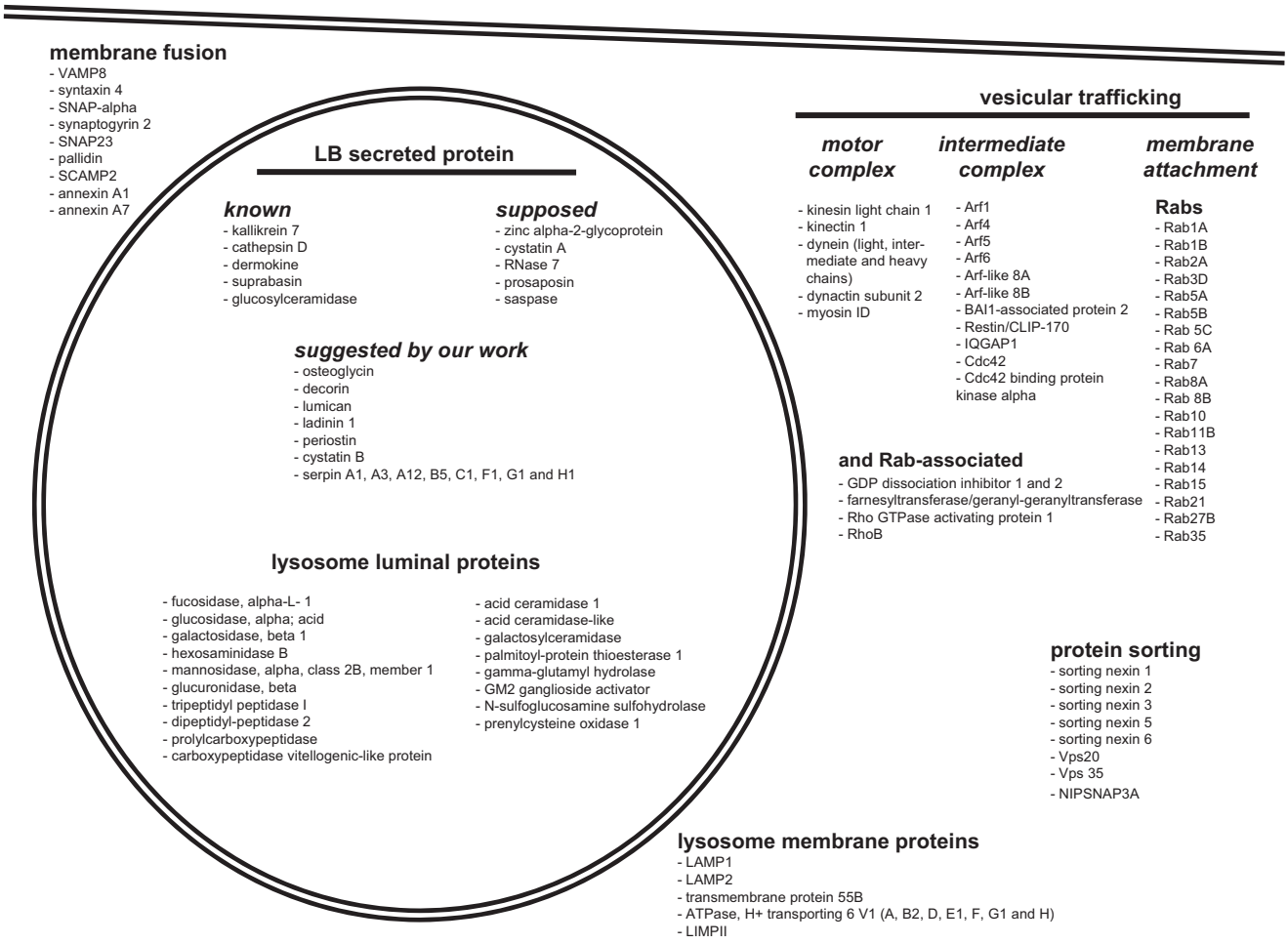

FIG. 8. **A functional model of LBs.** Among the 984 proteins identified in the epidermis LB-enriched fraction, we noted several proteins previously known or supposed to be secreted by LBs and several proteins previously localized in either the lumen or membrane of lysosomes in other tissues. We also proposed some of them to be secreted by LBs and others to be involved in LB trafficking because they have been previously involved in all steps of intracytoplasmic vesicular trafficking (motor complex, intermediate complex, and membrane attachment, including Rabs and Rab-associated proteins). Finally some identified proteins may play a role in the sorting of LB cargos and in the fusion between the LB membrane (*double circle*) and the plasma membrane (*double line*). The number of MS/MS queries and sequence coverage corresponding to the listed proteins are indicated in Table II except for kallikrein 7 (two matched peptides; 10% sequence coverage; gene name, *KLK7*) and acid ceramidase-like (two matched peptides; 10% sequence coverage; gene name, *ASAHL*; protein name, *N*-acylethanolamine-hydrolyzing acid amidase).

ponents of but have not been localized in LBs before this work. These are the zinc-α_2-glycoprotein (also known as desquamin), the function of which is unclear (53, 54); the retroviral-like aspartic protease saspase (55); the antimicrobial protein RNase7 (56); the protease inhibitor cystatin A (57); and prosaposin, which is involved in transport and maturation of sphingolipids (58).

We detected several extracellular matrix proteins: osteoglycin, decorin, lumican, ladinin 1, and periostin. Nothing is known about the secretion of extracellular matrix elements in the stratum granulosum, although the extracellular matrix is increasingly being considered as important for the properties and function of the stratum corneum (59). This identification leads us to suppose that LBs may be involved in the secretion of extracellular matrix components in the upper epidermis.

Proteins Potentially Involved in Desquamation—Among the proteins identified in the LB-enriched fraction, we found three proteins (two proteases, namely cathepsin D and kallikrein 7, and one member of a family of cathepsin inhibitors, namely cystatin A) already known to play a role in desquamation and 19 others that could also be implicated in this complex process. This is the case for cystatin B. Indeed cystatin M/E, another member of the family, has been detected in the upper layers of human epidermis and shown to be secreted by LBs in the intercorneocyte spaces where it is assumed to be involved in the control of desquamation (60, 61). This is also the case of six lysosomal glycosidases (a fucosidase, the α-glucosidase, β_1-galactosidase, β-glucuronidase, hexosaminidase B, and α-mannosidase). Secreted glycosidases are suspected to be involved in desquamation, and synergis-

tic activities of proteases and glycosidases have been demonstrated in the degradation of corneodesmosomes in the upper stratum corneum. They could hydrolyze the sugar moieties of the extracellular parts of corneodesmosome proteins, facilitating their proteolytic degradation (62, 63). However, the exact nature of the glycosidases present in the stratum corneum is not known. In addition, lysosomal peptidases identified in the LB proteome (tripeptidyl-peptidase I, dipeptidyl-peptidase II, vitellogenic carboxypeptidase-like protein, and prolyl carboxypeptidase) may also be secreted and involved, like the above discussed proteases, in the control of desquamation. Finally we identified eight serpins (serpins A1, A3, A12, B5, C1, F1, G1, and H1), members of a family of serine protease inhibitors (64). Serpins B2 and B5 have already been shown to be expressed in the granular layer of the epidermis, and serpin B2 is cross-linked to the cornified envelope by transglutaminase 1 (65, 66). Overexpression of serpin B2 has been observed in patients with Netherton syndrome (OMIM 256500), suggesting that it plays a role in desquamation. Therefore we propose that several serpins, including those we identified, are secreted by LBs and involved in the regulation of desquamation.

Proteins of Lysosomes—Epidermal LBs are considered to be lysosome-related organelles, so we paid attention to proteins previously localized in lysosomes. Confirming this relationship, we found lysosome luminal (17 in addition to cathepsin D and prosaposin) and membrane (11) proteins, including LAMP1 and LAMP2. In agreement with this evidence for their location in the epidermal LBs, LAMP1 and -2 have previously been described in the LBs of the lung (67). The acidic content of epidermal LBs has been highlighted previously (5), but the exact nature of H^+-ATPase involved in the maintenance of this acidic character had not been identified. In this study we distinguished seven subunits of the ATP6V1 proton pump that we propose as a good candidate for this function. We also found several glycosidases and peptidases that could take part in desquamation as discussed above. Also among the lysosomal proteins that we suggest are secreted by LBs, there are acid ceramidase 1 and a recently described acid ceramidase-like protein (again the latter protein was not automatically validated but was identified with a Mascot score of 46.8 and with MS/MS spectra shown in supplemental Fig. 2) that should take part in the catabolism of ceramides in the stratum corneum. Acidic ceramidase activity is preferentially localized within the lysosomal compartment in extracutaneous tissues (68). In the epidermis, an acidic ceramidase activity and acid ceramidase 1 have been described in the stratum corneum. Until now, based on the physicochemical properties of these enzymes, the ceramidase activity has been considered to be restricted to the extracellular space. Moreover the strong increase in acidic ceramidase activity observed during keratinocyte differentiation is not paralleled by a similar change in acid ceramidase 1-encoding mRNA (69). Although this discrepancy has been tentatively explained by post-transcriptional modifications, it may also result from the expression of another acid ceramidase, *i.e.* the acid ceramidase-like protein we identified. In addition, the galactosylceramidase present in the LB-enriched fraction has never been described in the epidermis and could play a role in the maturation of galactosylceramides in the stratum corneum (70).

Our results suggest that LBs could be considered as a specialized kind of secretory lysosomes. Lysosomes are the main degradative compartment within eukaryotic cells for misfolded trans-Golgi network-derived and cytosolic proteins. They also represent the end point of the endocytic pathway; the endocytosed material is either degraded or recycled back to the plasma membrane. However, some cell types contain lysosome-related organelles, also called secretory lysosomes, which secrete their contents into the extracellular spaces in response to external stimuli. These organelles share many characteristics with conventional lysosomes: an acidic luminal pH, many acid hydrolases, and the presence of LAMP proteins at their membrane but the absence of mannose 6-phosphate receptors. Various molecules are stored in the secretory lysosomes before their secretion according to the cell type: melanins in melanocytes, histamine in mast cells, perforin and granzymes in natural killer T cells, and clotting agents in platelets (71, 72). Another example of this specialization of secretory lysosomes can be found in osteoclasts, which are the cells responsible for the degradation of the organic and inorganic bone matrix during bone remodeling. When bone resorption is induced, osteoclasts migrate to the site of resorption and secrete the contents of their lysosome-related acidic vesicles. The mineral is dissolved by the acid, the collagen matrix is degraded by the proteinases, and then the degradation products are internalized for recycling (39). Our results indicate that epidermal LBs are of this type of secretory lysosomes.

Proteins Potentially Implicated in the Transport and Secretion of LBs—Among the proteins identified from the LB-enriched fraction, a number are suspected to be involved in vesicular trafficking, in particular the Rab family and Rab-associated proteins. Rab proteins in their GTP-bound form ensure a linkage between vesicle membranes and trafficking complexes recruiting effectors with high specificity to membrane compartments (73). Among the identified Rab proteins, we found Rab11 that was recently detected in the upper spinous and granular layers of human epidermis where it is associated with LBs (25), Rab3D previously implicated in the exocytosis of a subpopulation of LBs in alveolar epithelial type II cells (74), and Rab27B that regulates the secretion of the platelet secretory lysosomes (75). In this study, we focused on Rab7, a protein known to be localized in endo/lysosome-related vesicles (76, 77) and shown to control, together with Rac1, the transport of secretory lysosomes to the apical zone of the plasma membrane in bone-resorbing osteoclasts (39). We found that Rab7 was mainly expressed in the cytoplasm of granular keratinocytes where it was partially co-localized

with corneodesmosin by indirect immunofluorescence. Using immunoelectron microscopy, we also detected Rab7 in very close proximity with some LBs in human epidermis (data not shown). Rab7 could therefore be involved in some particular steps of LB secretion or in the secretion of a particular subpopulation of LBs. In agreement with this line of reasoning, in living A431 cells, the following of several Rabs tagged with green fluorescent protein and of transferrin as an endosomal cargo has shown that the Rab proteins are compartmentalized within the same continuous membrane of early endosomes, creating mosaics of different Rab domains through the recruitment of specific effector proteins (78).

We also identified proteins known to form intermediate complexes between vesicles and cytoskeletal elements such as the ADP-ribosylation factors (Arf1, -4, -5, and -6 and Arf-like 8A and 8B) (79). Proteins of the Arf family are believed to function as regulators of membrane trafficking in the secretory pathway (80). For example, Arf6 seems to be required for endosome recycling and has been shown to regulate actin modeling through the activation of Rac1 (81). Arf-like 8A and 8B have been localized to lysosomes in mammalian cells. Their overexpression results in microtubule-dependent redistribution of lysosomes toward the cell periphery, suggesting a role in lysosome transport (82). Detailed studies would be necessary to prove the implication of the identified Arf proteins in LB trafficking.

Motor proteins and some of their receptors implicated in the vesicular movements along the microtubules or actin filaments (kinesin light chain 1, kinectin 1, dynein components, dynactin 2, and myosin-Id) are present in the proteome of the LB-enriched fraction. This together with the presence of actin and tubulin subunits and also actin- and microtubule-associated proteins (supplemental Tables 1 and 3 and Table II) strongly suggests that LBs are routed in keratinocytes on microtubules and maybe microfilaments like other vesicles in other cells (83).

According to the "SNARE hypothesis," a model explaining the process and specificity of docking and fusion of vesicles to their target membranes during vesicular transport, membrane proteins from the donor vesicle (v-SNAREs or VAMPs) recognize and interact with proteins of the acceptor membrane (t-SNAREs or syntaxins). Once the two SNAREs are bound to each other, they recruit the general elements of the fusion apparatus, namely the *N*-ethylmaleimide-sensitive factor (NSF) and soluble NSF attachment proteins (SNAPs), to the site of membrane fusion. A mutation in *SNAP*29 causes a neurocutaneous syndrome called the cerebral dysgenesis, neuropathy, ichthyosis, and palmoplantar keratoderma (CEDNIK) syndrome (OMIM 609528), particularly characterized by an abnormal maturation of LB and, in consequence, a mislocation of epidermal lipids and proteases. The resulting ichthyotic phenotype suggests a crucial role for membrane fusion proteins in the epidermis barrier homeostasis (84). In this study, we found a v-SNARE, namely VAMP8, which is known to be implicated in the secretion of platelet (85) and mast cell (86) secretory lysosomes, and a t-SNARE, namely syntaxin 4. We also identified components of the fusion apparatus, the proteins SNAP-α, SNAP23, and palladin (87). Moreover we identified the SNAP23-associated transmembrane protein SCAMP2, which also plays a role in membrane fusion during exocytosis (88).

Proteins Potentially Implicated in the Sorting of LB Cargos—The sorting nexins constitute a large conserved family of hydrophilic molecules. Based on the functions of their yeast homologs, it has been suggested that mammalian sorting nexins ensure the proper delivery of organelle-specific proteins (89). Among the five sorting nexins we identified, sorting nexin-1 is particularly relevant for LB because it has been shown to play a role in targeting ligand-activated epidermal growth factor receptor to the lysosomes for its degradation (90). In yeast, the vacuolar protein sorting (Vps) proteins are involved in trafficking of endocytic and biosynthetic proteins to the vacuole, the fungal equivalent of the mammalian lysosomes. In association with sorting nexin-1 and -2 and other Vps proteins, human Vps35 is required to retrieve proteins from the endosomes to the late-Golgi network (91). Proteins of the sorting nexin and Vps families identified in the LB-containing fraction may be implicated in the biosynthetic sorting of LB cargos, but their exact function remains to be established as is the case for the NIPSNAP3A protein (92).

Evidence for a Role of CLIP-170 and Its Associated Proteins in the Trafficking and/or Secretion of LBs

Among the identified proteins that had previously been implicated in vesicular trafficking, we focused on a protein called restin/CLIP-170, a member of the cytoplasmic linker protein (CLIP) family, and on some of its effectors. CLIP-170 is known to mediate the linkage of vesicles to microtubules. It specifically accumulates at the plus ends of growing microtubules where it recruits dynactin that can then regulate the motor proteins dynein and kinesin (26). CLIP-170 has been reported to form a tripartite complex with IQGAP1 and Rac1/Cdc42 that appears to function as a linker between vesicles, microtubules, and cortical actin meshwork probably through Rab proteins (35, 39, 93). We were particularly interested in this protein for several reasons. (i) Microtubules have already been postulated to be involved in LB transport in epithelial pulmonary cells, and drug- or bacterial infection-induced changes in microtubules have been associated with changes in the metabolism of surfactant components (94). (ii) In cytotoxic T lymphocytes polarized after interaction with their target cells, secretory lysosomes move along microtubules toward the cell-cell contact sites. There their content is released into the so-called secretory cleft inducing the target cell death (95). (iii) Disruption of microtubules in human monocytes appears to impair lysosome exocytosis (96). We showed that, in human epidermis, CLIP-170 is expressed in the actual cells in which LBs are observed from the nuclear edge in the spinous

keratinocytes to the cell periphery in the upper granular layer. It is not expressed, or was not detected, in the basal and lower suprabasal keratinocytes. Although CLIP-170 is usually considered as a ubiquitously expressed protein, to our knowledge no exhaustive studies explore its expression in every tissue and cell type. Because it has not been detected in myocytes of heart muscle and in some glial cells (Human Protein Atlas), CLIP-170 expression may depend on cell type and differentiation state. Moreover on skin cryosections analyzed by confocal microscopy, the anti-CLIP-170 antibodies produced a punctate staining highly evocative of vesicles with a diameter compatible with that of LBs. We also demonstrated that CLIP-170 is co-localized with cathepsin D, a protease secreted via LBs (Fig. 5). Unfortunately we were not able to localize CLIP-170 at the ultrastructural level probably because, in immunoelectron microscopy, masking of the epitope recognized by the anti-CLIP-170 antibody takes place. In agreement with the location of CLIP-170 on LBs, a large number (>50) of the proteins we identified in the LB-enriched fractions, including Cdc42, Cdc42-binding protein kinase α, and BAI1-associated protein 2, are known to interact either directly or indirectly with CLIP-170 as highlighted using the knowledge-based software developed by Ingenuity Systems Inc. (Fig. 3). A majority of (84%), but not all, CLIP-170-positive vesicles were also stained by an anti-Cdc42 antibody (Fig. 6). Further confirming the interaction between CLIP-170 and Cdc42 in human epidermis, we observed that both proteins were co-immunoprecipitated from an epidermis extract by the anti-CLIP-170 antibody. Finally we found evidence that CLIP-170 was also partially co-localized with Rab7 (Fig. 6). These data strongly suggest that the three proteins form a complex at the membranes of cathepsin D-containing LBs and are probably involved in their trafficking and/or secretion. They may facilitate the transport of the vesicles along microtubules from the Golgi apparatus to the keratinocyte periphery. Because CLIP-170 seems not to be co-localized with corneodesmosin, another protein transported in LBs, it might be that CLIP-170 is implicated in the transport of a subpopulation of LBs. If true, this would confirm that LBs are a heterogeneous population of vesiculotubular structures. Indeed Ishida-Yamamoto *et al.* (4) have observed that the proteases and corneodesmosin are sorted independently as distinct aggregates. It has also been shown that the serine protease inhibitor lympho-epithelial kazal-related inhibitor is localized in LBs separated from its epidermis-specific target proteases KLK7 and KLK5 (97). In addition, the observation that a proportion of Cdc42 is co-localized with corneodesmosin and not with CLIP-170 suggests that all LBs are linked to Cdc42 independently of their binding by CLIP-170. It would be interesting to look for the presence of another member of the CLIP family on the CLIP-170-negative and corneodesmosin-positive LBs.

Surprisingly IQGAP1, which is expressed in the cytoplasm of all epidermal keratinocytes, was not found to be co-localized with CLIP-170, its described partner in other cell types (35) (Fig. 6*a*). However, anti-IQGAP1 antibody stained LBs both before and during secretion as observed by immunoelectron microscopy (data not shown). The potential implication of this multifunctional protein in LB secretion cannot be excluded but remains to be analyzed in more detail. In any case, it does not seem to be implicated in the CLIP-170·Cdc42 complex.

In conclusion, this study provides evidence that nano-LC-MS/MS combined with monodimensional separation constitutes a powerful method for identifying proteins in a complex mixture such as subcellular structures. It provides the first data on the complex molecular mechanisms involved in LB transport and secretion in the epidermis and highlights a new function for CLIP-170 in a complex with Cdc42 and/or Rab7. We also confirmed the existence of several subpopulations of epidermal LBs and suggest that different molecular complexes control their transport in the granular keratinocytes. Our data also indicate that epidermal LBs must be considered as secretory lysosomes. Further investigations on each protein identified will be necessary for a clear understanding of LB trafficking and secretion in the epidermis and more generally in other epithelia.

Acknowledgments—We thank Prof. J.-P. Chavoin for providing human skin; S. Allard (confocal microscopy facility, INSERM IFR30) for help with the confocal microscope; M.-P. Henri, M.-F. Isaïa, and C. Pons for technical assistance; and the "Centre de Microscopie Electronique Appliquée à la Biologie," University of Toulouse III, for the electron microscopy analysis. We thank Dr. M.-C. Méchin for critical reading of the manuscript.

* This study was supported in part by grants from the CNRS, including the "Programme Protéomique et génie des protéines, appel à propositions 2004"; the University Paul Sabatier-Toulouse III; the Génopole Toulouse Midi-Pyrénées et Région Midi-Pyrénées (to B. M.); the INSERM; the European Social Fund; and the European Regional Development Fund. The costs of publication of this article were defrayed in part by the payment of page charges. This article must therefore be hereby marked "*advertisement*" in accordance with 18 U.S.C. Section 1734 solely to indicate this fact.

S The on-line version of this article (available at http://www.mcponline.org) contains supplemental material.

§ Recipient of a fellowship from the French Ministry for Education, Research and Technology.

** To whom correspondence should be addressed: CNRS-UPS UMR5165, Faculté de Médecine, 37 allées Jules Guesde, 31073 Toulouse, France. Tel.: 33-5-61-14-59-48; Fax: 33-5-61-14-59-38; E-mail: msimon@udear.cnrs.fr.

REFERENCES

1. Madison, K. C. (2003) Barrier function of the skin: "la raison d'etre" of the epidermis. *J. Investig. Dermatol.* **121,** 231–241
2. Norlen, L. (2001) Skin barrier formation: the membrane folding model. *J. Investig. Dermatol.* **117,** 823–829
3. Grayson, S., Johnson-Winegar, A. G., Wintroub, B. U., Isseroff, R. R., Epstein, E. H., Jr., and Elias, P. M. (1985) Lamellar body-enriched fractions from neonatal mice: preparative techniques and partial characterization. *J. Investig. Dermatol.* **85,** 289–294
4. Ishida-Yamamoto, A., Simon, M., Kishibe, M., Miyauchi, Y., Takahashi, H., Yoshida, S., O'Brien, T. J., Serre, G., and Iizuka, H. (2004) Epidermal

lamellar granules transport different cargoes as distinct aggregates. *J. Investig. Dermatol.* **122,** 1137–1144
5. Chapman, S. J., and Walsh, A. (1989) Membrane-coating granules are acidic organelles which possess proton pumps. *J. Investig. Dermatol.* **93,** 466–470
6. Hayward, A. F. (1979) Membrane-coating granules. *Int. Rev. Cytol.* **59,** 97–127
7. Landmann, L. (1988) The epidermal permeability barrier. *Anat. Embryol.* (*Berl.*) **178,** 1–13
8. Menon, G. K., Ghadially, R., Williams, M. L., and Elias, P. M. (1992) Lamellar bodies as delivery systems of hydrolytic enzymes: implications for normal and abnormal desquamation. *Br. J. Dermatol.* **126,** 337–345
9. Madison, K. C., Sando, G. N., Howard, E. J., True, C. A., Gilbert, D., Swartzendruber, D. C., and Wertz, P. W. (1998) Lamellar granule biogenesis: a role for ceramide glucosyltransferase, lysosomal enzyme transport, and the Golgi. *J. Investig. Dermatol. Symp. Proc.* **3,** 80–86
10. Serre, G., Mils, V., Haftek, M., Vincent, C., Croute, F., Reano, A., Ouhayoun, J. P., Bettinger, S., and Soleilhavoup, J. P. (1991) Identification of late differentiation antigens of human cornified epithelia, expressed in reorganized desmosomes and bound to cross-linked envelope. *J. Investig. Dermatol.* **97,** 1061–1072
11. Nakane, H., Ishida-Yamamoto, A., Takahashi, H., and Iizuka, H. (2002) Elafin, a secretory protein, is cross-linked into the cornified cell envelopes from the inside of psoriatic keratinocytes. *J. Investig. Dermatol.* **119,** 50–55
12. Galliano, M. F., Toulza, E., Gallinaro, H., Jonca, N., Ishida-Yamamoto, A., Serre, G., and Guerrin, M. (2006) A novel protease inhibitor of the α2-macroglobulin family expressed in the human epidermis. *J. Biol. Chem.* **281,** 5780–5789
13. Gallo, R. L., and Nizet, V. (2003) Endogenous production of antimicrobial peptides in innate immunity and human disease. *Curr. Allergy Asthma Rep.* **3,** 402–409
14. Ganz, T. (2003) Defensins: antimicrobial peptides of innate immunity. *Nat. Rev. Immunol.* **3,** 710–720
15. Sando, G. N., Zhu, H., Weis, J. M., Richman, J. T., Wertz, P. W., and Madison, K. C. (2003) Caveolin expression and localization in human keratinocytes suggest a role in lamellar granule biogenesis. *J. Investig. Dermatol.* **120,** 531–541
16. Krawczyk, W. S., and Wilgram, G. F. (1975) The synthesis of keratinosomes during epidermal wound healing. *J. Investig. Dermatol.* **64,** 263–267
17. Ghadially, R., Reed, J. T., and Elias, P. M. (1996) Stratum corneum structure and function correlates with phenotype in psoriasis. *J. Investig. Dermatol.* **107,** 558–564
18. Werner, Y., Lindberg, M., and Forslind, B. (1987) Membrane-coating granules in "dry" non-eczematous skin of patients with atopic dermatitis. A quantitative electron microscopic study. *Acta Dermato-Venereol.* **67,** 385–390
19. Elias, P. M., Fartasch, M., Crumrine, D., Behne, M., Uchida, Y., and Holleran, W. M. (2000) Origin of the corneocyte lipid envelope (CLE): observations in harlequin ichthyosis and cultured human keratinocytes. *J. Investig. Dermatol.* **115,** 765–769
20. Kelsell, D. P., Norgett, E. E., Unsworth, H., Teh, M. T., Cullup, T., Mein, C. A., Dopping-Hepenstal, P. J., Dale, B. A., Tadini, G., Fleckman, P., Stephens, K. G., Sybert, V. P., Mallory, S. B., North, B. V., Witt, D. R., Sprecher, E., Taylor, A. E., Ilchyshyn, A., Kennedy, C. T., Goodyear, H., Moss, C., Paige, D., Harper, J. I., Young, B. D., Leigh, I. M., Eady, R. A., and O'Toole, E. A. (2005) Mutations in ABCA12 underlie the severe congenital skin disease harlequin ichthyosis. *Am. J. Hum. Genet.* **76,** 794–803
21. Odland, G. F., and Holbrook, K. (1981) The lamellar granules of epidermis. *Curr. Probl. Dermatol.* **9,** 29–49
22. Schmitz, G., and Muller, G. (1991) Structure and function of lamellar bodies, lipid-protein complexes involved in storage and secretion of cellular lipids. *J. Lipid Res.* **32,** 1539–1570
23. Dobbs, L. G. (1989) Pulmonary surfactant. *Annu. Rev. Med.* **40,** 431–446
24. Cheong, N., Madesh, M., Gonzales, L. W., Zhao, M., Yu, K., Ballard, P. L., and Shuman, H. (2006) Functional and trafficking defects in ATP binding cassette A3 mutants associated with respiratory distress syndrome. *J. Biol. Chem.* **281,** 9791–9800
25. Ishida-Yamamoto, A., Kishibe, M., Takahashi, H., and Iizuka, H. (2007) Rab11 is associated with epidermal lamellar granules. *J. Investig. Dermatol.* **127,** 2166–2170
26. Galjart, N. (2005) CLIPs and CLASPs and cellular dynamics. *Nat. Rev. Mol Cell. Biol.* **6,** 487–498
27. Simon, M., Montezin, M., Guerrin, M., Durieux, J. J., and Serre, G. (1997) Characterization and purification of human corneodesmosin, an epidermal basic glycoprotein associated with corneocyte-specific modified desmosomes. *J. Biol. Chem.* **272,** 31770–31776
28. Wilm, M., Shevchenko, A., Houthaeve, T., Breit, S., Schweigerer, L., Fotsis, T., and Mann, M. (1996) Femtomole sequencing of proteins from polyacrylamide gels by nano-electrospray mass spectrometry. *Nature* **379,** 466–469
29. Bouyssie, D., Gonzalez de Peredo, A., Mouton, E., Albigot, R., Roussel, L., Ortega, N., Cayrol, C., Burlet-Schiltz, O., Girard, J. P., and Monsarrat, B. (2007) Mascot file parsing and quantification (MFPaQ), a new software to parse, validate, and quantify proteomics data generated by ICAT and SILAC mass spectrometric analyses: application to the proteomics study of membrane proteins from primary human endothelial cells. *Mol. Cell. Proteomics* **6,** 1621–1637
30. Sondell, B., Thornell, L. E., and Egelrud, T. (1995) Evidence that stratum corneum chymotryptic enzyme is transported to the stratum corneum extracellular space via lamellar bodies. *J. Investig. Dermatol.* **104,** 819–823
31. Toulza, E., Galliano, M. F., Jonca, N., Gallinaro, H., Mechin, M. C., Ishida-Yamamoto, A., Serre, G., and Guerrin, M. (2006) The human dermokine gene: description of novel isoforms with different tissue-specific expression and subcellular location. *J. Investig. Dermatol.* **126,** 503–506
32. Adachi, J., Kumar, C., Zhang, Y., and Mann, M. (2007) In-depth analysis of the adipocyte proteome by mass spectrometry and bioinformatics. *Mol. Cell. Proteomics* **6,** 1257–1273
33. Andersen, J. S., Wilkinson, C. J., Mayor, T., Mortensen, P., Nigg, E. A., and Mann, M. (2003) Proteomic characterization of the human centrosome by protein correlation profiling. *Nature* **426,** 570–574
34. Simon, M., Jonca, N., Guerrin, M., Haftek, M., Bernard, D., Caubet, C., Egelrud, T., Schmidt, R., and Serre, G. (2001) Refined characterization of corneodesmosin proteolysis during terminal differentiation of human epidermis and its relationship to desquamation. *J. Biol. Chem.* **276,** 20292–20299
35. Fukata, M., Watanabe, T., Noritake, J., Nakagawa, M., Yamaga, M., Kuroda, S., Matsuura, Y., Iwamatsu, A., Perez, F., and Kaibuchi, K. (2002) Rac1 and Cdc42 capture microtubules through IQGAP1 and CLIP-170. *Cell* **109,** 873–885
36. Benitah, S. A., Frye, M., Glogauer, M., and Watt, F. M. (2005) Stem cell depletion through epidermal deletion of Rac1. *Science* **309,** 933–935
37. Zerial, M., and Stenmark, H. (1993) Rab GTPases in vesicular transport. *Curr. Opin. Cell Biol.* **5,** 613–620
38. Zerial, M., and McBride, H. (2001) Rab proteins as membrane organizers. *Nat. Rev. Mol. Cell Biol.* **2,** 107–117
39. Sun, Y., Buki, K. G., Ettala, O., Vaaraniemi, J. P., and Vaananen, H. K. (2005) Possible role of direct Rac1-Rab7 interaction in ruffled border formation of osteoclasts. *J. Biol. Chem.* **280,** 32356–32361
40. Presslauer, S., Hinterhuber, G., Cauza, K., Horvat, R., Rappersberger, K., Wolff, K., and Foedinger, D. (2003) RasGAP-like protein IQGAP1 is expressed by human keratinocytes and recognized by autoantibodies in association with bullous skin disease. *J. Investig. Dermatol.* **120,** 365–371
41. Yates, J. R., III, Gilchrist, A., Howell, K. E., and Bergeron, J. J. (2005) Proteomics of organelles and large cellular structures. *Nat. Rev. Mol. Cell Biol.* **6,** 702–714
42. Toulza, E., Mattiuzzo, N., Galliano, M.-F., Jonca, N., Dossat, C., Jacob, D., de Daruvar, A., Wincker, P., Serre, G., and Guerrin, M. (2007) Large-scale identification of human genes implicated in epidermal barrier function. *Genome Biol.* **8,** R107
43. Fielding, C. J., and Fielding, P. E. (2001) Cellular cholesterol efflux. *Biochim. Biophys. Acta* **1533,** 175–189
44. Langhorst, M. F., Reuter, A., and Stuermer, C. A. (2005) Scaffolding microdomains and beyond: the function of reggie/flotillin proteins. *CMLS Cell. Mol. Life Sci.* **62,** 2228–2240
45. Bared, S. M., Buechler, C., Boettcher, A., Dayoub, R., Sigruener, A., Grandl, M., Rudolph, C., Dada, A., and Schmitz, G. (2004) Association of ABCA1 with syntaxin 13 and flotillin-1 and enhanced phagocytosis in tangier cells. *Mol. Biol. Cell* **15,** 5399–5407

46. Liu, J., Deyoung, S. M., Zhang, M., Dold, L. H., and Saltiel, A. R. (2005) The stomatin/prohibitin/flotillin/HflK/C domain of flotillin-1 contains distinct sequences that direct plasma membrane localization and protein interactions in 3T3-L1 adipocytes. *J. Biol. Chem.* **280,** 16125–16134
47. Chi, A., Valencia, J. C., Hu, Z. Z., Watabe, H., Yamaguchi, H., Mangini, N. J., Huang, H., Canfield, V. A., Cheng, K. C., Yang, F., Abe, R., Yamagishi, S., Shabanowitz, J., Hearing, V. J., Wu, C., Appella, E., and Hunt, D. F. (2006) Proteomic and bioinformatic characterization of the biogenesis and function of melanosomes. *J. Proteome Res.* **5,** 3135–3144
48. Casey, T. M., Meade, J. L., and Hewitt, E. W. (2007) Organelle proteomics: identification of the exocytic machinery associated with the natural killer cell secretory lysosome. *Mol. Cell. Proteomics* **6,** 767–780
49. Williams, T. M., and Lisanti, M. P. (2004) The caveolin proteins. *Genome Biol.* **5,** 214
50. Gosens, R., Stelmack, G. L., Dueck, G., McNeill, K. D., Yamasaki, A., Gerthoffer, W. T., Unruh, H., Gounni, A. S., Zaagsma, J., and Halayko, A. J. (2006) Role of caveolin-1 in p42/p44 MAP kinase activation and proliferation of human airway smooth muscle. *Am. J. Physiol.* **291,** L523–L534
51. Razani, B., Rubin, C. S., and Lisanti, M. P. (1999) Regulation of cAMP-mediated signal transduction via interaction of caveolins with the catalytic subunit of protein kinase A. *J. Biol. Chem.* **274,** 26353–26360
52. Moffatt, P., Salois, P., St-Amant, N., Gaumond, M. H., and Lanctot, C. (2004) Identification of a conserved cluster of skin-specific genes encoding secreted proteins. *Gene* (*Amst.*) **334,** 123–131
53. Brysk, M. M., Lei, G., Rajaraman, S., Selvanayagam, P., Rassekh, C. H., Brysk, H., Tyring, S. K., and Arany, I. (1997) Gene expression of zinc-α2-glycoprotein in normal human epidermal and buccal epithelia. *In Vivo* **11,** 271–274
54. Lei, G., Arany, I., Tyring, S. K., Brysk, H., and Brysk, M. M. (1998) Zinc-α2-glycoprotein has ribonuclease activity. *Arch. Biochem. Biophys.* **355,** 160–164
55. Bernard, D., Mehul, B., Thomas-Collignon, A., Delattre, C., Donovan, M., and Schmidt, R. (2005) Identification and characterization of a novel retroviral-like aspartic protease specifically expressed in human epidermis. *J. Investig. Dermatol.* **125,** 278–287
56. Harder, J., and Schroder, J. M. (2002) RNase 7, a novel innate immune defense antimicrobial protein of healthy human skin. *J. Biol. Chem.* **277,** 46779–46784
57. Zeeuwen, P. L. (2004) Epidermal differentiation: the role of proteases and their inhibitors. *Eur J. Cell Biol.* **83,** 761–773
58. Choi, M. J., and Maibach, H. I. (2005) Role of ceramides in barrier function of healthy and diseased skin. *Am. J. Clin. Dermatol.* **6,** 215–223
59. Maytin, E. V., Chung, H. H., and Seetharaman, V. M. (2004) Hyaluronan participates in the epidermal response to disruption of the permeability barrier in vivo. *Am. J. Pathol.* **165,** 1331–1341
60. Cheng, T., Hitomi, K., van Vlijmen-Willems, I. M., de Jongh, G. J., Yamamoto, K., Nishi, K., Watts, C., Reinheckel, T., Schalkwijk, J., and Zeeuwen, P. L. (2006) Cystatin M/E is a high affinity inhibitor of cathepsin V and cathepsin L by a reactive site that is distinct from the legumain-binding site. A novel clue for the role of cystatin M/E in epidermal cornification. *J. Biol. Chem.* **281,** 15893–15899
61. Zeeuwen, P. L., Ishida-Yamamoto, A., van Vlijmen-Willems, I. M., Cheng, T., Bergers, M., Iizuka, H., and Schalkwijk, J. (2007) Colocalization of cystatin M/E and cathepsin V in lamellar granules and corneodesmosomes suggests a functional role in epidermal differentiation. *J. Investig. Dermatol.* **127,** 120–128
62. Walsh, A., and Chapman, S. J. (1991) Sugars protect desmosome and corneosome glycoproteins from proteolysis. *Arch. Dermatol. Res.* **283,** 174–179
63. Rawlings, A. V., and Harding, C. R. (2004) Moisturization and skin barrier function. *Dermatol. Ther.* **17,** Suppl. 1, 43–48
64. Law, R. H., Zhang, Q., McGowan, S., Buckle, A. M., Silverman, G. A., Wong, W., Rosado, C. J., Langendorf, C. G., Pike, R. N., Bird, P. I., and Whisstock, J. C. (2006) An overview of the serpin superfamily. *Genome Biol.* **7,** 216
65. Reis-Filho, J. S., Torio, B., Albergaria, A., and Schmitt, F. C. (2002) Maspin expression in normal skin and usual cutaneous carcinomas. *Virchows Arch.* **441,** 551–558
66. Oji, V., Oji, M. E., Adamini, N., Walker, T., Aufenvenne, K., Raghunath, M., and Traupe, H. (2006) Plasminogen activator inhibitor-2 is expressed in different types of congenital ichthyosis: in vivo evidence for its cross-linking into the cornified cell envelope by transglutaminase-1. *Br. J. Dermatol.* **154,** 860–867
67. Weaver, T. E., Na, C. L., and Stahlman, M. (2002) Biogenesis of lamellar bodies, lysosome-related organelles involved in storage and secretion of pulmonary surfactant. *Semin. Cell Dev. Biol.* **13,** 263–270
68. Ferlinz, K., Kopal, G., Bernardo, K., Linke, T., Bar, J., Breiden, B., Neumann, U., Lang, F., Schuchman, E. H., and Sandhoff, K. (2001) Human acid ceramidase: processing, glycosylation, and lysosomal targeting. *J. Biol. Chem.* **276,** 35352–35360
69. Houben, E., Holleran, W. M., Yaginuma, T., Mao, C., Obeid, L. M., Rogiers, V., Takagi, Y., Elias, P. M., and Uchida, Y. (2006) Differentiation-associated expression of ceramidase isoforms in cultured keratinocytes and epidermis. *J. Lipid Res.* **47,** 1063–1070
70. Hamanaka, S., Asagami, C., Suzuki, M., Inagaki, F., and Suzuki, A. (1989) Structure determination of glucosyl β1-N-(ω-O-linoleoyl)-acylsphingosines of human epidermis. *J. Biochem.* (*Tokyo*) **105,** 684–690
71. Holt, O. J., Gallo, F., and Griffiths, G. M. (2006) Regulating secretory lysosomes. *J. Biochem.* (*Tokyo*) **140,** 7–12
72. Dell'Angelica, E. C., Mullins, C., Caplan, S., and Bonifacino, J. S. (2000) Lysosome-related organelles. *FASEB J.* **14,** 1265–1278
73. Pfeffer, S. R. (2001) Rab GTPases: specifying and deciphering organelle identity and function. *Trends Cell Biol.* **11,** 487–491
74. van Weeren, L., de Graaff, A. M., Jamieson, J. D., Batenburg, J. J., and Valentijn, J. A. (2004) Rab3D and actin reveal distinct lamellar body subpopulations in alveolar epithelial type II cells. *Am. J. Respir. Cell Mol. Biol.* **30,** 288–295
75. Tolmachova, T., Abrink, M., Futter, C. E., Authi, K. S., and Seabra, M. C. (2007) Rab27b regulates number and secretion of platelet dense granules. *Proc. Natl. Acad. Sci. U. S. A.* **104,** 5872–5877
76. Feng, Y., Press, B., and Wandinger-Ness, A. (1995) Rab 7: an important regulator of late endocytic membrane traffic. *J. Cell Biol.* **131,** 1435–1452
77. Meresse, S., Gorvel, J. P., and Chavrier, P. (1995) The rab7 GTPase resides on a vesicular compartment connected to lysosomes. *J. Cell Sci.* **108,** 3349–3358
78. Sonnichsen, B., De Renzis, S., Nielsen, E., Rietdorf, J., and Zerial, M. (2000) Distinct membrane domains on endosomes in the recycling pathway visualized by multicolor imaging of Rab4, Rab5, and Rab11. *J. Cell Biol.* **149,** 901–914
79. Chen, J. L., Xu, W., and Stamnes, M. (2005) In vitro reconstitution of ARF-regulated cytoskeletal dynamics on Golgi membranes. *Methods Enzymol.* **404,** 345–358
80. Volpicelli-Daley, L. A., Li, Y., Zhang, C. J., and Kahn, R. A. (2005) Isoform-selective effects of the depletion of ADP-ribosylation factors 1–5 on membrane traffic. *Mol. Biol. Cell* **16,** 4495–4508
81. D'Souza-Schorey, C., and Chavrier, P. (2006) ARF proteins: roles in membrane traffic and beyond. *Nat. Rev. Mol. Cell Biol.* **7,** 347–358
82. Hofmann, I., and Munro, S. (2006) An N-terminally acetylated Arf-like GTPase is localised to lysosomes and affects their motility. *J. Cell Sci.* **119,** 1494–1503
83. Karcher, R. L., Deacon, S. W., and Gelfand, V. I. (2002) Motor-cargo interactions: the key to transport specificity. *Trends Cell Biol.* **12,** 21–27
84. Sprecher, E., Ishida-Yamamoto, A., Mizrahi-Koren, M., Rapaport, D., Goldsher, D., Indelman, M., Topaz, O., Chefetz, I., Keren, H., O'Brien, T. J., Bercovich, D., Shalev, S., Geiger, D., Bergman, R., Horowitz, M., and Mandel, H. (2005) A mutation in SNAP29, coding for a SNARE protein involved in intracellular trafficking, causes a novel neurocutaneous syndrome characterized by cerebral dysgenesis, neuropathy, ichthyosis, and palmoplantar keratoderma. *Am. J. Hum. Genet.* **77,** 242–251
85. Polgar, J., Chung, S. H., and Reed, G. L. (2002) Vesicle-associated membrane protein 3 (VAMP-3) and VAMP-8 are present in human platelets and are required for granule secretion. *Blood* **100,** 1081–1083
86. Paumet, F., Le Mao, J., Martin, S., Galli, T., David, B., Blank, U., and Roa, M. (2000) Soluble NSF attachment protein receptors (SNAREs) in RBL-2H3 mast cells: functional role of syntaxin 4 in exocytosis and identification of a vesicle-associated membrane protein 8-containing secretory compartment. *J. Immunol.* **164,** 5850–5857
87. Falcon-Perez, J. M., and Dell'Angelica, E. C. (2002) The pallidin (Pldn) gene and the role of SNARE proteins in melanosome biogenesis. *Pigm. Cell Res.* **15,** 82–86
88. Castle, J. D., Guo, Z., and Liu, L. (2002) Function of the t-SNARE SNAP-23

and secretory carrier membrane proteins (SCAMPs) in exocytosis in mast cells. *Mol. Immunol.* **38,** 1337–1340
89. Haft, C. R., de la Luz Sierra, M., Barr, V. A., Haft, D. H., and Taylor, S. I. (1998) Identification of a family of sorting nexin molecules and characterization of their association with receptors. *Mol. Cell. Biol.* **18,** 7278–7287
90. Kurten, R. C., Cadena, D. L., and Gill, G. N. (1996) Enhanced degradation of EGF receptors by a sorting nexin, SNX1. *Science* **272,** 1008–1010
91. Seet, L. F., and Hong, W. (2006) The Phox (PX) domain proteins and membrane traffic. *Biochim. Biophys. Acta* **1761,** 878–896
92. Buechler, C., Bodzioch, M., Bared, S. M., Sigruener, A., Boettcher, A., Lapicka-Bodzioch, K., Aslanidis, C., Duong, C. Q., Grandl, M., Langmann, T., Dembinska-Kiec, A., and Schmitz, G. (2004) Expression pattern and raft association of NIPSNAP3 and NIPSNAP4, highly homologous proteins encoded by genes in close proximity to the ATP-binding cassette transporter A1. *Genomics* **83,** 1116–1124
93. Stamnes, M. (2002) Regulating the actin cytoskeleton during vesicular transport. *Curr. Opin. Cell Biol.* **14,** 428–433
94. Wissel, H., Schulz, C., Rüdiger, M., Krüll, M., Stevens, P. A., and Waver, R. R. (2003) Chlamydia pneumoniae affect surfactant trafficking and secretion due to changes of type II cell cytoskeleton. *Am. J. Respir. Cell Mol. Biol.* **29,** 303–313
95. Stinchcombe, J. C., and Griffiths, G. M. (2007) Secretory mechanisms in cell-mediated cytotoxicity. *Annu. Rev. Cell Dev. Biol.* **23,** 495–517
96. Carta, S., Tassi, S., semino, C., Fossati, G., Mascagni, P., Dinarello, C. A., and Rubartelli, A. (2006) Histone deacetylase inhibitors prevent exocytosis of interleukin-1β-containing secretory lysosomes: role of microtubules. *Blood* **108,** 1618–1626
97. Ishida-Yamamoto, A., Deraison, C., Bonnart, C., Bitoun, E., Robinson, R., O'Brien, T. J., Wakamatsu, K., Ohtsubo, S., Takahashi, H., Hashimoto, Y., Dopping-Hepenstal, P. J., McGrath, J. A., Iizuka, H., Richard, G., and Hovnanian, A. (2005) LEKTI is localized in lamellar granules, separated from KLK5 and KLK7, and is secreted in the extracellular spaces of the superficial stratum granulosum. *J. Investig. Dermatol.* **124,** 360–366